AGE OF STRATOSPHERIC AIR: THEORY, OBSERVATIONS, AND MODELS

Darryn W. Waugh
Department of Earth and Planetary Sciences
Johns Hopkins University
Baltimore, Maryland, USA

Timothy M. Hall
NASA Goddard Institute for Space Studies
New York, New York, USA

Received 3 April 2001; revised 29 April 2002; accepted 4 November 2002; published 31 December 2002.

[1] We review the relationship between tracer distributions and transport timescales in the stratosphere and discuss the use of timescales to evaluate and constrain theories and numerical models of the stratosphere. The "age spectrum," the distribution of transit times since stratospheric air last made tropospheric contact, provides a way to understand the transport information of tracers, how sensitive different tracers are to various transport processes, and how to use tracers in combination to constrain transport rates. Trace gas observations can be used to infer aspects of the age spectrum, most commonly the "mean age," but also the shape of the spectrum. Observational inferences of transport timescales provide stringent tests of numerical models independent of photochemistry, and comparisons of these observations with chemical transport models have highlighted certain problems with transport in the models. Age simulations and comparisons with data can now be considered standard tests of stratospheric models. *INDEX TERMS:* 0341 Atmospheric Composition and Structure: Middle atmosphere—constituent transport and chemistry (3334); 0340 Atmospheric Composition and Structure: Middle atmosphere—composition and chemistry; 3334 Meteorology and Atmospheric Dynamics: Middle atmosphere dynamics (0341, 0342); 3362 Meteorology and Atmospheric Dynamics: Stratosphere/troposphere interactions; *KEYWORDS:* stratosphere, transport, tracers, age
Citation: Waugh, D. W., and T. M. Hall, Age of stratospheric air: Theory, observations, and models, *Rev. Geophys.*, *40*(4), 1010, doi: 10.1029/2000RG000101, 2002.

1. INTRODUCTION

[2] Transport is the movement of constituents and properties of a fluid by the fluid flow. Transport plays a crucial role in distributing climatically important trace constituents in the atmosphere and ocean. In the atmosphere many trace gases have regions of production and destruction that are well separated, and thus the distribution and evolution of these trace gases are determined by a complex interplay of sources, chemistry, and transport. In the stratosphere, the focus of this review, photochemical rates of important trace gases vary strongly with height and latitude. For example, chlorofluorocarbons (CFCs), nitrous oxide (N_2O), and methane (CH_4), which are greenhouse gases and source gases for molecules that destroy ozone, enter the stratosphere from the troposphere in the tropics but are not chemically broken down until they reach the middle stratosphere. Thus transport through the stratosphere largely determines the chemical lifetimes of these trace gases. Another example of the dominant role of transport is the distribution of ozone (O_3): It is chemically formed in the tropical middle stratosphere but is transported to high-latitude lower stratosphere where there is weak chemical destruction and where it thus displays its peak concentration. Hence understanding, quantifying, and modeling stratospheric transport is crucial for understanding and predicting the chemical evolution of the stratosphere.

[3] One summary of transport in the stratosphere and other geophysical domains is the distribution of elapsed times (transit times or "ages") for fluid to travel from one point or region to another. An infinitesimal fluid element small enough to maintain its integrity against mixing for all timescales of interest has a unique transit time. However, only properties averaged over the many fluid elements in a macroscopic fluid parcel are observable. In the presence of mixing the transport pathways from the specified source region to the position of the parcel may vary widely, and there is an associated distribution of transit times (an "age spectrum") since the parcel was last at the source region. The age spectrum has several features that make it an appealing descriptor of transport: (1) Considered as a function of both source and response points, the age spectrum contains complete information on the fluid transport. (2) Although the age spectrum cannot be observed directly, information on the age spectrum can be obtained from observable tracers. (3) Once estimated or simulated, the age spectrum can be used straightforwardly to determine the

8755-1209/02/2000RG000101*$15.00*

distribution and evolution of passive and inert tracers that cannot be measured directly.

[4] Two examples of point 3, the use of the age spectrum to infer tracer concentrations, are particularly important for understanding ozone depletion and climate change. In the stratosphere, chlorine, whose sources are primarily CFCs, is the major agent of O_3 destruction, and monitoring the evolution of atmospheric chlorine in response to international treaties is critical for understanding O_3 depletion and eventual recovery. In the stratosphere, chlorine exists in several chemical forms, and it is difficult to measure them all to obtain "total chlorine." However, the age spectrum has proved an effective way to estimate the evolution of total chlorine in the stratosphere [e.g., *Waugh et al.*, 2001]. Another important (nonstratospheric) application of the age spectrum concept is the ocean uptake of carbon. The ocean takes up a significant fraction of anthropogenic CO_2 from the atmosphere, but once in the ocean the carbon cannot easily be separated from background levels, and thus there is large uncertainty in the ocean distribution and total abundance of anthropogenic carbon. Recent work suggests that the age spectrum can be estimated from observable ocean tracers with sufficient accuracy to allow improved estimates of the distribution of anthropogenic carbon [*Hall et al.*, 2002].

[5] In addition to these general advantages, there are features of the circulation of the stratosphere that make the age spectrum and its mean (the "mean age") particularly useful for the analysis of stratospheric transport. In order to appreciate this utility, however, a brief review of the stratospheric circulation is necessary. On seasonal and longer timescales, stratospheric circulation can be effectively described in the latitude-height plane averaged around latitude circles (the "zonally averaged" circulation). Air and trace gases enter the stratosphere through the tropical tropopause, rise slowly within the tropical stratosphere, spread poleward primarily toward the winter pole, and descend in middle and high latitudes, where they reenter the troposphere (see Figure 1). This meridional circulation is known as the "Brewer-Dobson" circulation, after *Brewer* [1949] and *Dobson* [1956], who proposed it to explain the observed stratospheric distributions of ozone, water vapor, and other trace gases. The Brewer-Dobson circulation is the net meridional and vertical motion of air mass and includes the effects of both mean meridional winds and eddies, which differ from each other in magnitude and even sign [e.g., *Andrews et al.*, 1987]. The Brewer-Dobson circulation applies to material entering the stratosphere above ~18 km in the tropics; below this level, there is considerable direct exchange with the extratropical tropopause by a variety of mechanisms [e.g., *Holton et al.*, 1995].

[6] The timescale to travel around the Brewer-Dobson circulation is several years. In addition to this slow circulation, there is rapid quasi-horizontal (isentropic) transport and mixing in the middle latitudes of the winter hemisphere by "breaking" planetary-scale Rossby

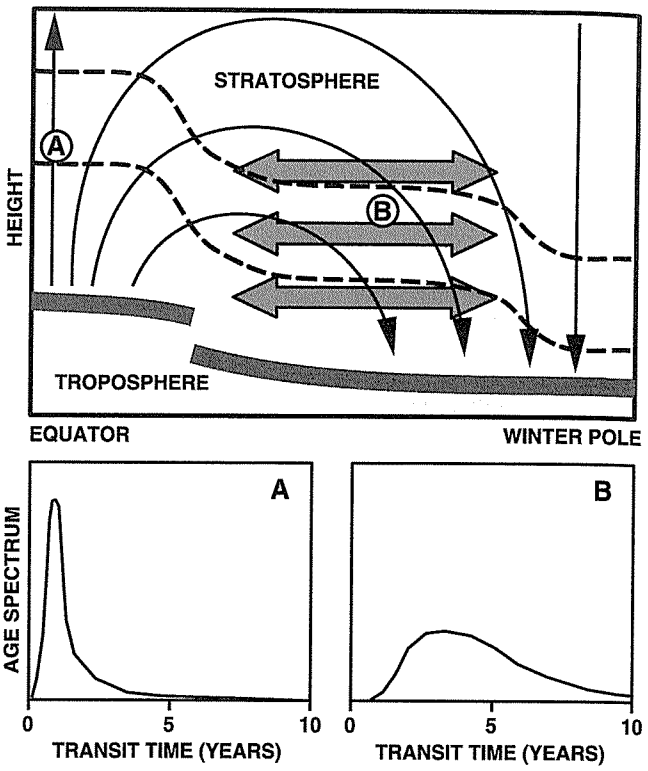

Figure 1. Schematic diagram of stratospheric circulation and typical age spectra. The thin solid curves represent the advective "Brewer-Dobson" circulation, the shaded double-headed arrows represent the quasi-horizontal wave-driven mixing, and the dashed curves represent isopleths of long-lived tracers. The bottom plots show typical age spectra in the tropics (location A) and extratropics (location B).

waves. As Rossby waves propagate up from the troposphere through wintertime stratospheric westerlies, their amplitudes increase [*Andrews et al.*, 1987]. The waves break when their amplitudes becomes sufficiently large. Rossby wave breaking results in quasi-horizontal overturning and mixing (in contrast to vertical overturning and mixing of internal gravity waves) [*McIntyre and Palmer*, 1983]. The wave breaking also deposits momentum and plays a major role in driving the Brewer-Dobson circulation [e.g., *Holton et al.*, 1995].

[7] The slow meridional circulation and the more rapid wave mixing are the dominant mechanisms determining the large-scale time-averaged distribution of stratospheric tracers [*Mahlman et al.*, 1986; *Holton*, 1986; *Plumb and Ko*, 1992]. The meridional circulation tends to elevate tracer isopleths in the tropics and lower them in high latitudes, while the wave mixing tends to homogenize the tracer mixing ratios along the quasi-horizontal surfaces (isentropes). The effects approximately balance, resulting in the tracer isopleth shape shown schematically in Figure 1. Both transport processes vary seasonally and interannually in magnitude and structure, producing corresponding variations in the tracer distributions.

[8] This picture of the stratospheric circulation pro-

vides the basic geometry of the large-scale transport but not the transport rates. Tracer observations are excellent tools to constrain these rates, as tracers are sensitive to transport mechanisms on all scales, many of which cannot be sufficiently sampled by direct wind measurements. Age-related concepts, in turn, are useful for interpreting tracer observations in terms of tracer-independent quantities. This is particularly true in the analysis of stratospheric transport. The source region of most stratospheric trace gases, the troposphere, is rapidly mixed by convection, baroclinic instability, and boundary layer turbulence, processes that are absent in the stratosphere. Consequently, spatial gradients of long-lived tracers are much smaller in the troposphere then in the stratosphere, and stratospheric trace gas distributions, and mean age and other diagnostics inferred from these distributions, are largely independent of the geographical distribution of tropospheric sources. In addition, because air and trace gases enter the stratosphere through a limited region in the tropics, the entire stratosphere can be considered as "downstream" of a single region. Thus stratospheric tracers of tropospheric origin respond to a time-dependent but spatially localized and homogeneous lower boundary condition. Contrast this to the more complex situation for ocean tracers of atmospheric origin. Such tracers are transported from surface waters to the deep ocean in several geographic regions, each with distinct tracer concentrations due to spatial variations in solubility. Hence it is often necessary to decompose deep ocean waters into components, each with different age characteristics [*Haine and Hall*, 2002].

[9] In this paper we review the theoretical, observational, and modeling aspects of the age of stratospheric air. The concept of age was first applied to the stratosphere by *Kida* [1983], who performed particle trajectory studies with a general circulation model (GCM). He recognized the utility of a statistical treatment of stratospheric transport and coined the term "age spectrum" for the transit time distributions of the particles. *Hall and Plumb* [1994] later developed the age spectrum mathematically, identifying it as a type of Green's function that propagates information of tropospheric variation of a tracer into the stratosphere. We review the theoretical aspects of the age and its statistical distribution in section 2. On the observational side, *Bischof et al.* [1985], using whole air samples of CO_2 from balloons, inferred the mean age in northern midlatitudes from the troposphere-to-stratosphere lag time in the trend in CO_2. These observations were expanded by *Schmidt and Khedim* [1991]. In recent years, there have been a large number of observational campaigns that have provided high-quality estimates of mean age and other related timescales. These observational inferences are reviewed in section 3. Simultaneously, many modeling studies have exploited the stratospheric age spectrum and mean age as a transport diagnostic. For example, in the NASA Models and Measurements II (MM2) study, simulations of the age spectrum and transient tracers from more than 20 models were compared to each other and to observations. In section 4 we review numerical simulations of mean age and other transport timescales. As discussed above, one application of the age spectrum is to infer tracer concentrations (such as total chlorine in the stratosphere). We discuss the relationship between mean age and different tracers in section 5.

[10] Before focusing on the stratosphere we note that age has a long history as a diagnostic of transport in a wide range of settings. In geophysical systems, age-related concepts have been used extensively to summarize the passage of material (e.g., carbon) through coupled zero-dimensional "reservoirs" [e.g., *Erickson*, 1971; *Bolin and Rhode*, 1973; *Nir and Lewis*, 1975; *O'Neill et al.*, 1994]. Earlier work in "reservoir theory" appears in chemical engineering and has been widely applied in this field [e.g., *Danckwerts*, 1953; *Levenspiel*, 1972]. More recently, oceanographers and hydrologists have used concepts similar to stratospheric scientists to describe ocean and groundwater transport rates. The concept of mean age, the mean time since a water mass last made contact with the surface, has been used in oceans (where it is known as the idealized age tracer) [*England*, 1995] and groundwater [*Goode*, 1996], as has the more general concept of transit time distributions (age spectra) [*Beining and Roether*, 1996; *Deleersnijder et al.*, 2001; *Etcheverry and Perrochet*, 2000; *Haine and Hall*, 2002; *Khatiwala et al.*, 2001; *Varni and Carrera*, 1998]. Common to these systems is the advective-diffusive nature of the transport. Superposed on bulk advective flow are random (or pseudorandom) motions, which necessitate a statistical description of transport times.

2. THEORY

2.1. Age Spectrum

[11] Because of the irreversible mixing that occurs in the stratosphere, properties of an air parcel acquired at previous times and various locations (e.g., the mixing ratio of a tracer) are most naturally described as means over statistical distributions. For convenience we refer to a small but finite-sized air mass as a "parcel," and we consider the parcel to consist of an infinitude of infinitesimal and irreducible "fluid elements" that maintain their integrity against mixing for all timescales of interest. Only properties averaged over all the parcel's fluid elements are observable. One property of a fluid element in a stratospheric parcel is the elapsed time since it was last in the troposphere. The distribution of the fluid elements by their time since last troposphere contact is known as the "age spectrum" [*Kida*, 1983], and the average over the distribution is known as the "mean age."

[12] From our understanding of stratospheric transport (discussed in section 1) we expect the shape of the age spectrum to vary within the stratosphere, as illus-

trated schematically in figure 1. In the tropical lower stratosphere, mixing has had little chance to dilute parcels with older air from other stratospheric regions, and large-scale zonally averaged transport occurs primarily by vertical advection. The spectrum is strongly peaked near the time for vertical ascent from the tropopause (location A in figure 1). In contrast, in the middle- and high-latitude lower stratosphere and throughout the upper stratosphere, mixing provides a multiplicity of pathways from the tropopause with an associated range of transit times, and consequently the age spectrum is broad (location B in Figure 1).

[13] A mathematical formulation of the age spectrum was first presented by *Hall and Plumb* [1994] (hereinafter HP94). They identified the age spectrum as a type of Green's function that propagates a boundary condition on tracer mixing ratio from a specified region Ω (e.g., the Earth's surface or the tropical tropopause) into the stratosphere. Consider the continuity equation for a conserved and passive tracer of mixing ratio $\chi(r, t)$:

$$\frac{\partial \chi}{\partial t} + \mathcal{L}(\chi) = 0, \qquad (1)$$

where $\mathcal{L}$ is a linear transport operator. (The linearity of the transport operator is equivalent to the passiveness of the tracer. No assumptions are made about stationarity.) The tracer's mixing ratio $\chi(\Omega, t)$ is assumed to be known as a function of time in a region Ω, and the stratospheric mixing ratio is considered as a response. This is equivalent to specifying a boundary condition for χ on Ω. The response at point r in the stratosphere is

$$\chi(r, t) = \int_{-\infty}^{t} \chi(\Omega, t')\mathcal{G}(r, t|\Omega, t')dt', \qquad (2)$$

where $\mathcal{G}(r, t|\Omega, t')$ satisfies (1) with the boundary condition $\mathcal{G}(r_s, t|\Omega, t) = \delta(t - t')$ for r_s on Ω. $\mathcal{G}(r, t|\Omega, t')$ "propagates" mixing ratios on Ω at time t' to the point r at time t. It weights the contributions from Ω at various past times t' to the present time mixing ratio at r. $\mathcal{G}$ depends on two time variables, a generalization of HP94, who only considered stationary transport. Rewriting $\mathcal{G}$ as $\mathcal{G}(r, t|\Omega, t - \xi)$, where $\xi = t - t'$ is the elapsed time, one has the age spectral interpretation: $\mathcal{G}\delta\xi$ is the mass fraction of the air parcel at location r and time t that was last in contact with the region Ω an elapsed time ξ to $\xi + \delta\xi$ ago. For stationary transport, $\mathcal{G}$ depends only on ξ. More realistically, transport varies in time (e.g., seasonally or interannually), and $\mathcal{G}$ also depends explicitly on t. In what follows, we generally take a time-averaged perspective, suppressing the t dependence.

[14] It is worth digressing to make two points about the formulation represented by equation (2). Strictly, equation (2) is only true if χ is uniform over Ω. More generally, χ must be convolved with a spatially varying $\mathcal{G}$ over Ω. This is a minor approximation for the stratospheric air above around 18 km (the "overworld") because, as discussed in section 1, tracers enter the stratosphere through a limited geographic region, the tropical tropopause, regardless of their tropospheric history and surface distribution. Consequently, variations in the definition of Ω within the troposphere only cause uniform offsets to χ in the overworld. However, spatial dependence of surface χ may be visible in the extratropical stratosphere below 19 km [*Ray et al.*, 1999].

[15] A more general point concerns the approach of using mixing ratio boundary conditions. Considering the tracer mixing ratio in the stratosphere as a response to a prescribed mixing ratio history at the surface is physically reasonable, as the stratosphere plays little direct role itself in fixing the tracer's near-surface abundance. However, in other settings (e.g., CO_2 in the troposphere) it is more physical to consider the mixing ratio as a response to explicit tracer sources rather than mixing ratio boundary conditions. In this way, no solution is assumed anywhere, and transport plays its natural role in determining the tracer mixing ratio throughout the atmosphere, including in the region of the sources. Recently, *Holzer and Hall* [2000] have generalized the work of HP94 in order to relate the transit time distribution to the consideration of explicit sources rather than mixing ratio boundary conditions. In addition to the distribution of transit times at location r since last Ω contact (the age spectrum), their framework encompasses distributions of transit times from r to first Ω contact. Related approaches have been taken by *Deleersnijder et al.* [2001].

2.2. Propagation of Transient Tracers

[16] Given the age spectra and the time history of a conserved passive tracer on Ω, one can compute the tracer distribution and evolution throughout the stratosphere. Conversely, it is often possible to infer aspects of the stratospheric age spectrum from stratospheric measurements of transient tracers and knowledge of their history on Ω.

[17] For the special case of bulk advection without mixing the age spectrum at a location r is a delta function peaked at the time $\tau_{adv}(r)$ for the flow to carry tracer along a streamline from Ω to r. Expression (2) reduces to $\chi(r, t) = \chi(\Omega, t - \tau_{adv}(r))$, where $\tau_{adv}(r)$ is independent of the time variation of χ on Ω. In other words, all transient signals at Ω are simply carried into the stratosphere unchanged, except for a lag of τ_{adv}. More generally, with mixing present, there is a range of transit times from Ω to r, the age spectrum is not a delta function, and tracers with different time variations on Ω have different responses at r. In certain cases it is still possible to define a lag time, but its magnitude will generally depend on the nature of the time variation at Ω.

[18] One such case in which a lag time τ can be defined is a conserved tracer whose concentration χ on Ω is monotonically increasing (or decreasing) with time. The concentration time lag τ is the elapsed time between the occurrence of a particular mixing ratio at a location r and its occurrence at Ω

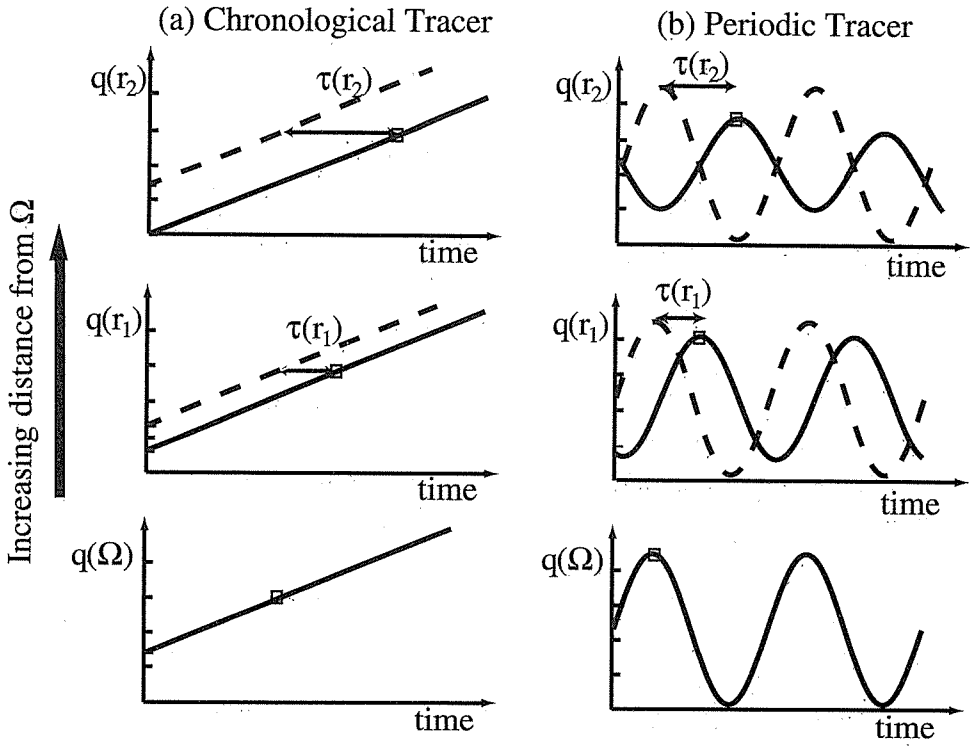

Figure 2. Schematic diagram of the time series of (a) monotonically increasing and (b) periodic tracers at two distances from the source region (tropical tropopause) Ω. Dashed curves correspond to time series at Ω.

$$\chi(r, t) = \chi(\Omega, t - \tau), \tag{3}$$

as illustrated in Figure 2a. In general, τ depends on the time history of $\chi(\Omega)$. (The exception is, as discussed above, pure advection, where $\tau = \tau_{adv}$ whatever the time dependence of $\chi(\Omega, t)$.) A special case, however, is linear time variation of $\chi(\Omega, t)$, in which case τ is independent of the rate of linear variation, regardless of the nature of the transport, that is, regardless of the shape of the age spectrum. Substituting $\chi(\Omega, t) \propto t$ into equation (2) one finds that the time lag is

$$\tau(r) = \int_0^\infty \xi \mathcal{G}(r|\Omega, \xi) d\xi \equiv \Gamma(r), \tag{4}$$

where Γ is the first moment of the age spectrum or the "mean age" (HP94). In other words, by measuring χ at point r, and going back through the tropospheric record to find the lag time for a match, one obtains the mean age.

[19] No real tracer exhibits exactly linear growth (or decline). Whether the tracer's lag time approximates the mean age depends on the degree to which the growth is linear over the width of the age spectrum. A tracer whose growth (or decay) in time is exponential ($e^{\sigma t}$) has, to first order in σ, a concentration time lag [*Varni and Carrera*, 1998; HP94]

$$\tau_{exp}(r) \approx \Gamma(r) - \sigma^{-1} \ln (1 + \sigma^2 \Delta^2(r)), \tag{5}$$

where Δ is the "age spectral width,"

$$\Delta^2(r) = \frac{1}{2} \int_0^\infty (\xi - \Gamma(r))^2 \mathcal{G}(r|\xi) d\xi, \tag{6}$$

a measure of the spread of transit times since the parcel at r had last troposphere contact. (In the special case of pure advective flow, $\Delta = 0$.) If $\sigma\Delta \ll 1$, the equation (5) reduces to

$$\tau_{exp}(r) \approx \Gamma(r) - \sigma \Delta^2(r). \tag{7}$$

From equation (7) we have $\tau_{exp} \approx \Gamma$ if the growth rate satisfies $\sigma^{-1} \gg \Delta^2/\Gamma$. HP94 found $\Delta^2/\Gamma \sim 0.7$ year through most of the stratosphere of a version of the Goddard Institute for Space Studies (GISS) stratospheric GCM, so $\tau_{exp} \sim \Gamma$ to within 10% for $\sigma^{-1} > 7$ years. The value of Δ^2/Γ varies considerably among stratospheric models, with, for example, the National Center for Atmospheric Research (NCAR) Middle Atmosphere version of the Community Climate Model version 2 (MACCM2) displaying a relatively uniform value of ~1.5 years [*Hall and Waugh*, 1997a]. Although the time lag of exponentially growing conserved tracers is not equivalent to Γ, using model estimates of Δ^2/Γ it is possible to account for this difference and use slowly nonlinearly varying tracers to estimate Γ [*Volk et al.*, 1997].

[20] For rapid nonlinear time variation in $\chi(\Omega)$, such as an annually periodic tracer signal, the age spectrum is typically wide enough that the troposphere-to-stratosphere lag time does not approximate the mean age.

Nonetheless, the distributions of such tracers still contain information on stratospheric transport. In fact, responses to time variations that are sufficiently different over the width of the age spectrum can be used in combination to place strong constraints on theories and rates of stratospheric transport. To explore this further, consider as a second class of tracers those whose mixing ratios vary periodically (with period $2\pi/\omega$). One can define a phase lag time $\tau_\omega(r)$ from the lag time of a maximum (or minimum) in the time series at stratospheric location r from that at Ω (Figure 2b). From equation (2) we have

$$A_\omega(r)e^{-i\omega\tau_\omega(r)} = \int_0^\infty e^{-i\omega\xi}\mathcal{G}(r|\Omega, \xi)d\xi, \qquad (8)$$

where A_ω is the amplitude of the oscillation. In the absence of mixing $\mathcal{G} = \delta(t - \tau_{adv}(r))$, so that $A_\omega(r) = 1$ and $\tau_\omega(r) = \tau_{adv}(r) = \Gamma(r)$ for all r. However, with mixing, $\tau_\omega \approx \Gamma$ only if $\omega\Delta^2/\Gamma \ll 1$, which is not generally true in the stratosphere for annually periodic signals.

[21] The above results show that in general the propagation of tracer mixing ratio signals into the stratosphere differs for different tropospheric time variation. The sensitivity to the tropospheric time variation depends on the shape of the age spectrum, which, in turn, depends on the relative rates of bulk advection and mixing.

[22] We illustrate this first by considering simple one-dimensional flow with constant advective velocity u and diffusivity k for Fickian diffusion. For this flow the age spectrum at position x is

$$\mathcal{G}(\Gamma, \Delta, t) = \frac{1}{2\Delta\sqrt{\pi\hat{t}^3}}\exp\left[\frac{-\Gamma^2(\hat{t}-1)^2}{4\Delta^2\hat{t}}\right], \qquad (9)$$

where $\Gamma = x/u$, $\Delta = \sqrt{kx/u^3}$, and $\hat{t} = t/\Gamma$. (The k independence of Γ is peculiar to this one-dimensional (1-D) model; more generally, as seen below, mean age is affected by mixing.) Distributions of the form (9) are known as inverse Gaussian distributions, and they have been used in many different fields to describe time distributions [e.g., *Chhikara and Folks*, 1989; *Seshadri*, 1999]. Figure 3a shows the age spectra for several values of spectral width Δ with mean age Γ fixed. (Note that $\Gamma^2/\Delta^2 = ux/k$ corresponds to the Peclet number of the flow. For fixed Γ an increasing Δ corresponds to decreasing Peclet number and increasing role of diffusion relative to advection.) For small Δ, transport is dominated by advection, and the spectrum is narrow and peaked near the mean age ($\Delta = 0$ corresponds to no diffusion and a delta function age spectrum at $t = \Gamma$). As Δ is increased (diffusion increased), the spectrum broadens, has a peak (modal time) at transit times increasingly shorter than the mean age, and develops an increasingly longer "tail" of old air.

[23] The impact of the different spectral shape on tracer timescales is shown in Figure 3b, where τ_{exp} (for $\sigma^{-1} = 4$ and 10 years) and τ_ω (for periodic tracers with an annual and a 3 year cycle) are plotted against Δ. (See *Hall and Plumb* [1994] for analytical formulae for these time lags.) For narrow spectra the timescales Γ, τ_ω, and τ_{exp} collapse to a single value; whereas when the spectra are broad, the three timescales differ significantly, with $\tau_\omega < \tau_{exp} < \Gamma$. In fact, for skewed spectra with a long tail of old transit times (a general property of diffusive-advective systems) it is always true that τ_{exp} and τ_ω are less than the mean age [*Hall and Waugh*, 1997a; *Deleersnijder et al.*, 2001]. The difference between the τ_ω and Γ can be understood by considering the contribution of the tail region to the two timescales: The tail contributes strongly to the mean age, but it represents several complete annual cycles at roughly equal magnitude, which

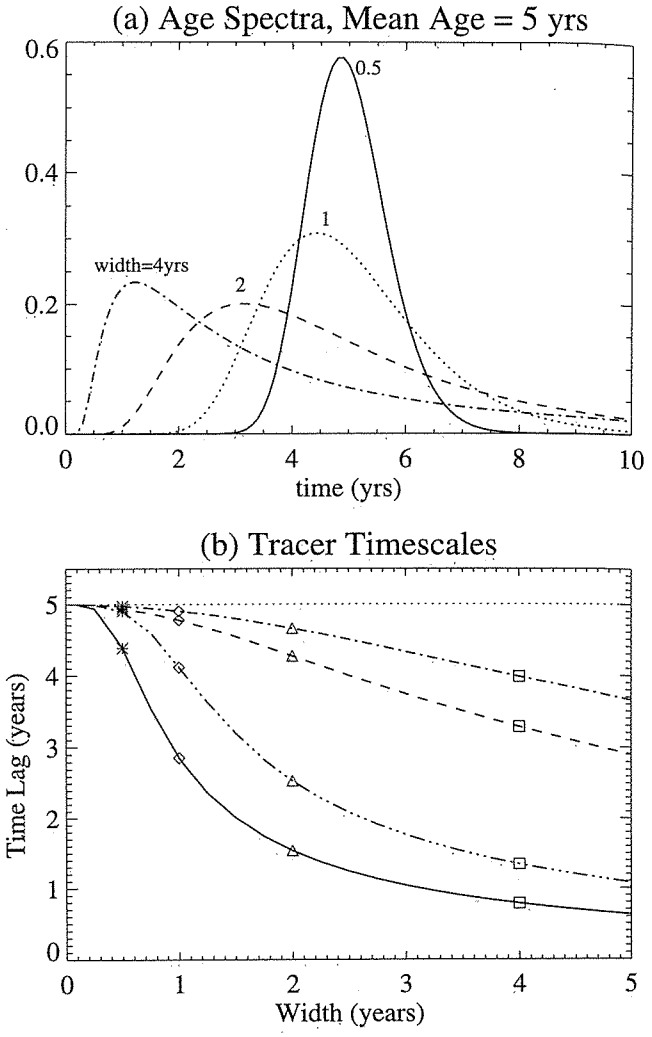

Figure 3. (a) Age spectra for one-dimensional advection-diffusion model with mean age $\Gamma = 5$ years and spectral width $\Delta = 0.5$ (solid curve), 1 (dotted curve), 2 (dashed curve), and 4 (dot-dashed curve) years. (b) Variation of τ_{exp}, for $\sigma^{-1} = 4$ (dashed curve) and 10 (dot-dashed curve) years and τ_ω for periodic tracers with an annual (solid curve) and a 3-year cycle (dot-dot-dot-dashed curve), with Δ for $\Gamma = 5$ years. The symbols correspond to time lags for spectra shown in Figure 3a.

thereby cancel. As a result, the net signal is biased toward the age spectral peak, which, if narrow enough, "picks out" a phase. The relationship $\tau_\omega < \Gamma$ is borne out both by observations (see section 3.4) and multidimensional models (see section 4.4).

[24] $\mathcal{G}$ given by equation (9) is also the age spectrum for 1-D diffusion and no advection in air with an $e^{-z/H}$ density variation, where H is a constant density scale height and z is the height (substitution of $u = k/H$ in equation (9) yields the form of $\mathcal{G}$ for 1-D mass-weighted diffusion given by HP94). This model has been applied to the stratosphere in the past. If rapid wave-induced quasi-horizontal (isentropic) mixing extended across all latitudes (the "global diffusor" limit), then, in fact, effective vertical transport would reduce to a 1-D diffusive model [*Plumb and Ko*, 1992]. However, numerous observations show that the tropics are relatively isolated from the rapid mixing of winter midlatitudes [*Trepte et al.*, 1993; *Murphy et al.*, 1993; *Randel et al.*, 1994; *Grant et al.*, 1996], so that the global stratosphere is poorly represented by a 1-D model.

[25] The simplest model that includes the partial isolation of the tropics is the "tropical leaky pipe" model [*Plumb*, 1996; *Neu and Plumb*, 1999], composed of three 1-D regions of vertical motion representing the tropics (upwelling) and horizontally well-mixed northern and southern midlatitudes (downwelling). The regions are coupled by the tropical outflow consistent with the divergent upwelling and by independently specified two-way tropical-midlatitude mixing. Vertical diffusion can be applied in each region. Figure 4 shows the age spectra and the mean age in the tropics and midlatitudes at height $2H$ above the tropopause as the transport processes are "turned on" one at a time. In Figure 4a, only advection is present, resulting in a tropical delta function and a midlatitude distribution of transit times corresponding to different "up-and-over" heights. With tropical-midlatitude mixing added (Figure 4b), the advective spike is still present in the tropics, but its magnitude is weaker, and there is a "tail" due to midlatitude air of various ages mixing back into the tropics. This air also lengthens the midlatitude tail because of recirculation. (See Appendix A of *Hall* [2000] for analytic expressions.) Small vertical diffusion (Figure 4c) broadens the advective spike and slightly reduces the mean age. At this stage the age spectra are qualitively similar to the 1-D advective-diffusive spectra, having an early peak and long tail, but their spectral peaks are more pronounced. Note that if one specifies a realistic velocity profile in the tropics with a minimum in the lower stratosphere [e.g., *Mote et al.*, 1998], one obtains a minimum in the tropical divergence, a separation of tropical outflow regions results, and midlatitude age spectra become bimodal. (Bimodal spectra have, in fact, been inferred from tracer observations [*Andrews et al.*, 2001a], as discussed in section 3.5.)

[26] The qualitative characteristics of the age spectra for the idealized 1-D model and the tropical leaky pipe model are similar to those of two-dimensional (2-D) and three-dimensional (3-D) numerical models. For example, Figure 5 shows zonally averaged age spectra from a three-dimensional chemical transport model (CTM) driven by winds from the NCAR MACCM2 model. Spectra from other models display similar characteristics [*Hall et al.*, 1999; *Park et al.*, 1999]. As in the case of the idealized models, the age spectra from the CTM are asymmetric with long tails. Moreover, the variation with location is consistent with the expectation illustrated in Figure 1: The spectra are most narrow, and peaked at earliest transit times, in the lower tropical stratosphere and are broad and shifted to longer transit times elsewhere.

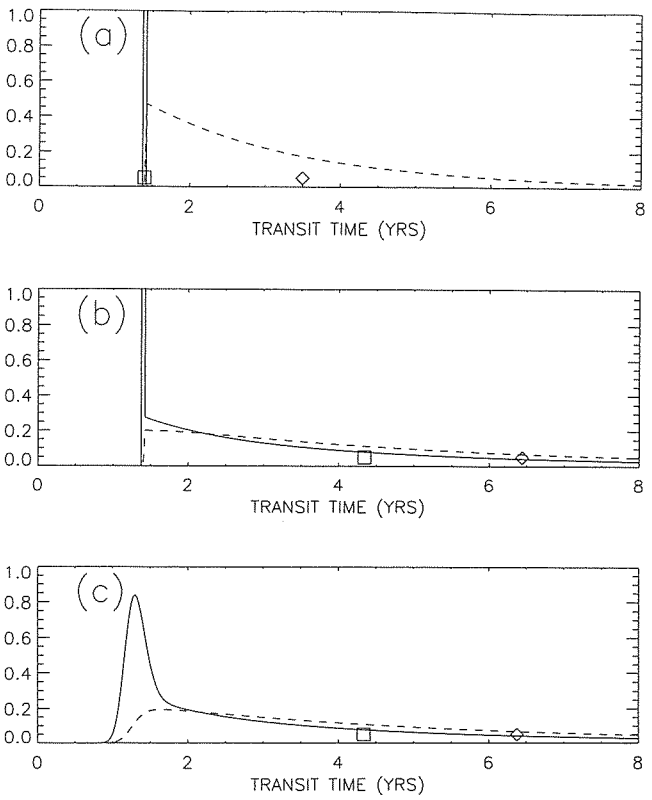

Figure 4. Age spectra for tropical leaky pipe model evaluated at $Z = 2H$ in tropics (solid) and midlatitudes (dashed). (a) The tropical upwelling rate $W = 0.3$ mm/s, timescale for tropical-midlatitude mixing $\tau = \infty$, and the vertical diffusivity $K = 0$; (b) $W = 0.3$ mm/s, $\tau = 1.0$ years, $K = 0$; (c) $W = 0.3$ mm/s, $\tau = 1.0$ years, $K = 0.1$ m^2/s. Symbols along the horizontal axis indicate mean age in the tropics (squares) and midlatitudes (triangles).

2.3. Further Issues

[27] The discussion so far applies to conservative tracers. Aspects of the age spectrum framework can be extended to include tracers undergoing photochemical evolution (e.g., $\mathcal{G}$ in equation (2) modified to include the effect of chemical losses) [*Volk et al.*, 1997; *Hall and Waugh*, 1998; *Plumb et al.*, 1999; *Schoeberl et al.*, 2000]. With photochemical loss in the stratosphere the time lag

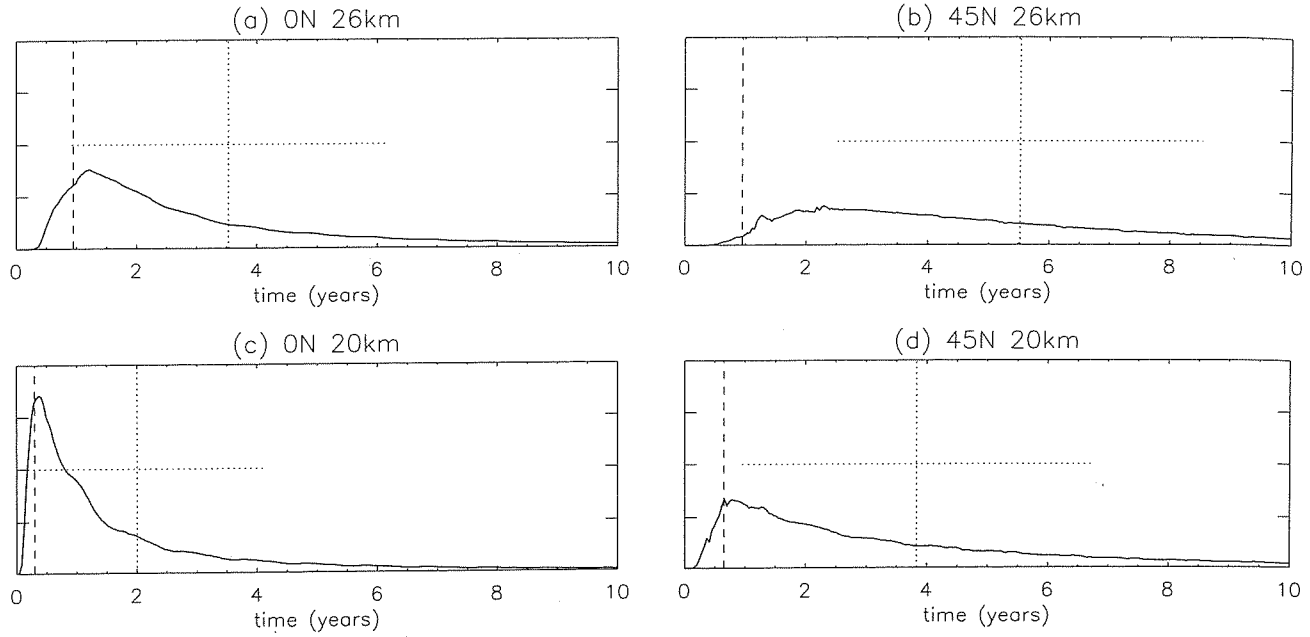

Figure 5. The age spectra for the three-dimensional chemical transport model driven by fields from National Center for Atmospheric Research Middle Atmosphere version of the Community Climate Model version 2 (MACCM2) [*Waugh et al.*, 1997] at four locations: the equator at 20 and 26 km and 45°N at 20 and 26 km. The mean age is indicated by the vertical dotted lines, the width is indicated by the horizontal dotted lines, and the phase lag of an annual cycle is indicated by the vertical dashed lines.

for a tracer with increasing tropospheric trend will be greater than the true mean age; one must go back further in the tropospheric record for a mixing ratio match. If some loss process is not known or not taken into account, then the tracer lag time will be an overestimate of the mean age. Even seemingly very slow photochemical loss, or loss only in the mesosphere, may noticeably affect lower stratospheric mean age inferences, as the mean age strongly weights fluid elements that have been in the stratosphere longest and that are therefore most likely to have traversed more photochemically active regions [*Hall and Waugh*, 1998]. Mesospheric photochemical loss processes may explain certain discrepancies between Γ inferred from different transient tracers, see section 3.2.

[28] Before moving on to observations and numerical simulations of stratospheric mean age and related quantities, it is worth noting an alternative but equivalent definition of mean age, more common in oceanographic applications. The "ideal age" τ_{id} is defined as the steady state solution to

$$\frac{\partial \tau_{id}}{\partial t} + \mathcal{L}(\tau_{id}) = 1 \qquad (10)$$

with a boundary condition of $\tau_{id} = 0$ at the surface [e.g., *Thiele and Sarmiento*, 1990; *England*, 1995] (also see *Goode* [1996] for application to groundwater flow). If one takes the first moment ($\int_0^\infty dt' t'$) of equation (1) for $\mathcal{G}$ with the surface boundary condition $\delta(t)$, one obtains precisely equation (10), demonstrating the equivalence of "mean age" Γ and the "ideal age" τ_{id}. This equivalence was noted by *Boering et al.* [1996], and *Neu and Plumb* [1999] have made use of formulation (10) to solve and analyze mean age in the tropical leaky pipe model of stratosphere transport. See *Hall and Haine* [2002] for further discussion.

[29] The mean age can also be related to eigenmodes of stratospheric transport, a concept developed in the context of coupled chemical species by *Prather* [1997]. As discussed by *Park et al.* [1999], for long transit times the age spectra at all locations decay exponentially at the same rate, i.e., $\mathcal{G}(x, t) \sim \psi_0(x) e^{-t/\tau_0}$ as $t \to \infty$. The decay rate τ_0 corresponds to the e-folding time of the longest-lived mode of stratospheric transport. Because Γ is strongly influenced by the tail region of $\mathcal{G}$, we expect a close connection between $\Gamma(x, t)$, $\psi_0(x, t)$, and τ_0. This was confirmed by examination of models in the MM2 study [*Park et al.*, 1999], which showed that for most models the spatial structure of Γ and τ_0 are very similar and that the variation of τ_0 among models is very similar to the variation of Γ.

3. OBSERVATIONS

[30] Determining the shape of the age spectra in the stratosphere would go a long way to quantifying the relative rates of advection and mixing. Unfortunately, the age spectra cannot be directly observed. However, as discussed in section 2 tracer-independent transport

TABLE 1. Observational Estimates of Mean Age in the 25–30 km and 55–60 km Ranges[a]

Latitude	*Period*	*Gas*	Γ, *(years)*	*Reference*
		25–30 km		
7°S	February 1997, November 1997	CO_2	3.5[b]	*Andrews et al.* [2001b]
7°S	February 1997, November 1997	SF_6	4.0[b]	*Ray et al.* [1999]
17°N	April 1987	SF_6	4.3	*Patra et al.* [1997]
17°N	March 1994	SF_6	4.7	*Harnisch et al.* [1996]
34°N	September 1996, May 1998	CO_2	5.5[b]	*Andrews et al.* [2001b]
34°N	September 1996, May 1998	SF_6	6.0[b]	*Ray et al.* [1999]
34°N	September 1993	HF	4–5	*Sen et al.* [1996]
40°N	May–September 1985–1991	CO_2	4.5	*Nakazawa et al.* [1995]
44°N	September 1993	SF_6	4.5	*Harnisch et al.* [1996]
44°N	September–November 1979–1984	CO_2	5.2	*Bischof et al.* [1985]
44°N	March–November 1976–1989	CO_2	5.6	*Schmidt and Khedim* [1991]
44°N	June 1997	CO_2, SF_6	6	*Strunk et al.* [2000]
65°N	June 1997 (V)	CO_2	5.5 (6)[b]	*Andrews et al.* [2001b]
65°N	June 1997 (V)	SF_6	6.0 (8)[b]	*Ray et al.* [1999]
68°N	January–February 1990 (V)	CO_2	2.3	*Schmidt and Khedim* [1991]
68°N	January–March 1991–1992, 1995 (V)	SF_6	6 (8–10)	*Harnisch et al.* [1996]
68°N	December 1988, January–March 1991–1992 (V)	CF_4	(7.5)	*Harnisch et al.* [1999]
68°N	February 1997	CO_2, SF_6	6	*Strunk et al.* [2000]
		55–60 km		
global	1992–1995	HF, HCl	4.7, 5.3	*Anderson et al.* [2000]
several	1985, 1992, 1993, 1994	HF	5–6	*Gunson et al.* [1996]
68°N	May 1987, December 1988	CF_4	11	*Harnish et al.* [1998]

[a]See Figure 6a for estimates at 20 km from aircraft observation [*Elkins et al.*, 1996; *Boering et al.*, 1996]. Numbers inside parentheses correspond to measurements inside polar vortex (V).
[b]Ages are relative to the tropical tropopause (other ages are relative to the surface).

timescales, and aspects of the age spectra, can be extracted from the propagation of transient tracers. Furthermore, indirect estimates of the age spectra have recently been made from tracer measurements. Here we discuss observations of such tracers and the resulting estimates of transport timescales. We first focus on estimates of the mean age and then on other aspects of the age spectrum.

3.1. Mean Age

[31] The mean age Γ can be calculated from measurements of a tracer that is conserved and whose concentration varies linearly with time over the width of the age spectrum (see equations (3) and (4)). (The tropical tropopause is often used as a reference for computing lag times at stratospheric locations. In this way, spatial variations within the troposphere do not introduce ambiguity when comparing mean ages from different tracers.) There are several chemical species that approximately satisfy the criterion of linear variation. Carbon dioxide (CO_2) is very long-lived, and its annual mean concentration has been increasing roughly linearly [*Conway et al.*, 1994], and hence it can be used to estimate the mean age. (Note that methane oxidation is a stratospheric source of CO_2, but this can accurately be accounted for when using CO_2 to calculate the mean age [*Woodbridge et al.*, 1995; *Boering et al.*, 1996].) Sulfur hexafluoride (SF_6) is also extremely long-lived (it is inert in the troposphere and stratosphere and has an estimated global lifetime of 800–3200 years [*Ravishankara et al.*, 1993; *Morris et al.*, 1995]), and its surface concentration growth is sufficiently close to linear [*Maiss et al.*, 1996; *Geller et al.*, 1997]. Two other fluorinated species, CF_4 and C_2F_6, have extremely long global lifetimes (greater than 50,000 and 10,000 years, respectively [*Ravishankara et al.*, 1993]) and are also possible chronological tracers, although their tropospheric histories are less well known than SF_6. During the 1980s the abundance of several CFCs was increasing at a near-linear rate, and measurements of these have been used to infer the mean age. However, as CFCs have significant stratospheric losses, these estimates are biased (as discussed in section 2.3), and we do not consider them here. It is also possible to calculate the mean age from conserved families of gases whose total abundance varies linearly. The tropospheric abundance of total fluorine (F_{tot}) and total chlorine (Cl_{tot}) increased approximately linearly in the 1980s and early 1990s, and the mean age may be estimated from measurements of these families during this period.

[32] Unfortunately, there are no observations of these trace gas species or families covering the whole stratosphere, and therefore global observations of Γ are not available. However, there is a growing number of measurements from balloon, aircraft, and space-borne platforms that can be combined to provide good coverage of Γ in the lower stratosphere and partial coverage in the middle and upper stratosphere. These measurements are summarized in Table 1.

[33] Before discussing the observational estimates of Γ, it is important to note several sources of possible error

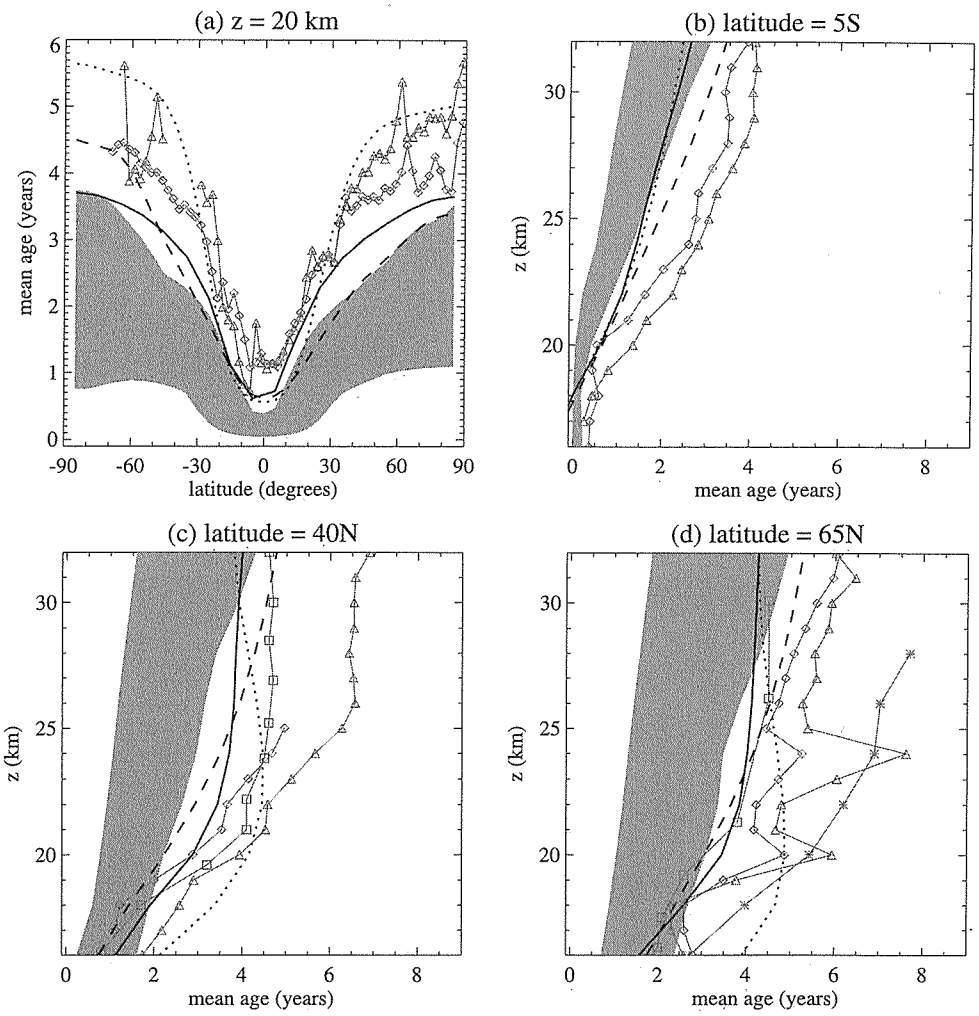

Figure 6. Comparison of observed (red curves with symbols) and modeled (blue shaded area and curves) mean age: (a) $z = 20$ km and latitude of (b) 5°S, (c) 40°N, and (d) 65°N. The shaded region indicates the range of most models in the Models and Measurements II (MM2) study, while the individual curves represent several models falling outside the range. The symbols represent observations: mean age from in situ CO_2 (diamonds) [*Boering et al.*, 1996; *Andrews et al.*, 2001b], in situ SF_6 (triangles) [*Elkins et al.*, 1996; *Ray et al.*, 1999], and whole air samples of SF_6 (square outside vortex and asterisk inside vortex) [*Harnisch et al.*, 1996]. See *Hall et al.* [1999] for details. See color version of this figure at back of this issue.

in mean age inferences. As discussed in section 2, nonlinearity in the tropospheric growth rate introduces error. There is a weak nonlinearity in the growth of SF_6 [e.g., *Geller et al.*, 1997] which introduces an uncertainty in estimates of Γ from SF_6 (see equation (5) and related discussion). *Volk et al.* [1997], using model-based estimates of the width of the age spectrum, estimated the effect on Γ to be ~0.5 years for Γ older than 4 years. The annual cycle in CO_2, if unaccounted for, introduces error in estimates of Γ from CO_2. This uncertainty is large within the tropical lower stratosphere but is much smaller elsewhere [*Hall and Prather*, 1993; *Boering et al.*, 1996]. There are also interannual variations in CO_2 growth, but *Andrews et al.* [2001b] showed that errors associated with both seasonal and interannual variations in CO_2 are insignificant for air with $\Gamma > 2$ years. Another source of error is the neglect of photochemical processes. As discussed in section 2, neglect of loss processes will result in an overestimate of Γ. As SF_6 and CO_2 both have mesospheric losses, neglect of these losses introduces a bias into the Γ estimates. The magnitude of this error in the stratosphere, discussed further in section 3.2, is only significant in the lower and middle stratosphere inside the winter polar vortex. Finally, imperfect knowledge of the time history of a tracer at the tropical tropopause introduces further uncertainty in the inferred mean age.

[34] In spite of these uncertainties, there is generally good agreement among different Γ estimates. This can be seen be comparing the entries in Table 1. Further comparisons are shown in Figure 6 which shows estimates of Γ from in situ measurements of CO_2 and SF_6 (red curves with diamonds and triangles, respectively) on the same platforms. (The red curves with asterisks and

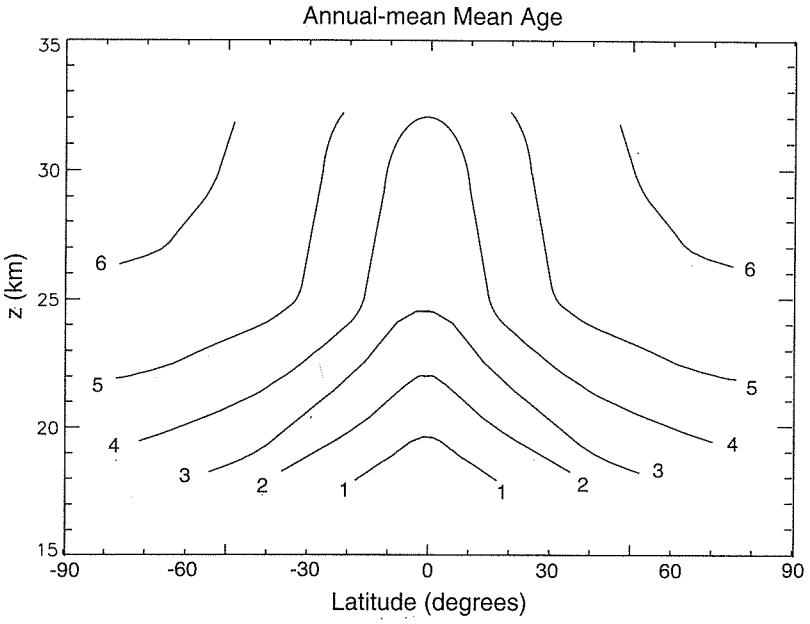

Figure 7. Schematic diagram of the altitude-latitude distribution of the annually averaged zonal mean of mean age based on vertical profiles from observations listed in Table 1 and ER-2 measurements around 20 km (e.g., Figure 6a). As it is based almost exclusively on Northern Hemisphere data, the schematic is hemispherically symmetric.

crosses show ages from whole air SF_6 samples from different balloon flights [*Harnsich et al.*, 1996], and the blue shaded regions and curves show model Γ and will be discussed later.) Figure 6a shows the latitudinal variation of Γ at 20 km from CO_2 and SF_6 measurements made aboard the NASA ER-2 aircraft during the period 1992–1997 [*Boering et al.*, 1996; *Elkins et al.*, 1996]. Both estimates of Γ show values around 1 year near the equator, large gradients in the subtropics, and values around 4–5 years at high latitudes. Figures 6b–6d show vertical profiles from Observations of Middle Stratosphere (OMS) balloon flights [*Andrews et al.*, 2001b; *Ray et al.*, 1999] in the tropics, middle latitudes, and high latitudes. There is again good agreement between the two estimates of Γ. At all latitudes, Γ increases with altitude with only weak vertical gradients above 25 km (the spikes in the high-latitude profiles, Figure 6d, are due to sampling of fragments of vortex air; see below).

[35] More detailed comparisons of Γ from the simultaneous measurements of CO_2 and SF_6 have been performed by *Strunk et al.* [2000] and *Andrews et al.* [2001b]. Both these studies showed good agreement between SF_6 and CO_2 ages except within polar vortex air, where Γ from SF_6 can be greater than that from CO_2 by 2 or more years. An example of this is shown in Figure 6d where the spikes in the OMS mean age profiles are due to sampling remnants of old polar vortex air [e.g., *Herman et al.*, 1998], and in these remnants Γ from SF_6 is significantly larger than that from CO_2. More recent measurements inside the 1999–2000 Arctic vortex confirm this bias between Γ from SF_6 and CO_2 (J. Elkins and A. Andrews, personal communication, 2000). These differences are probably due to unaccounted mesospheric SF_6 loss and are discussed further in section 3.2.

[36] One exception to the overall agreement is the study of *Harnisch et al.* [1998], which showed significant differences between Γ from SF_6 and CO_2 for whole air samples from a series of balloon flights. As an explanation, *Harnisch et al.* [1998] suggested that covariance between seasonality in surface CO_2 source and transport from the surface to the tropical tropopause could lead to a rectified stratospheric CO_2 signal not present for SF_6. However, this does not explain why the *Harnisch et al.* [1998] CO_2 profiles have different shapes than SF_6 profiles. Moreover, scatterplots of their CO_2 data versus N_2O are not compact, even while their SF_6-N_2O scatterplots are compact. A noncompact CO_2-N_2O relationship contradicts theoretical understanding of stratospheric transport [*Plumb and Ko*, 1992] and is not observed in other studies [*Boering et al.*, 1996; *Strunk et al.*, 2000; *Andrews et al.*, 2001b]. *Strunk et al.* [2000] suggested that an alternative explanation of the different ages is contamination of the CO_2 whole air samples.

[37] The estimates of Γ from the different measurements listed in Table 1 (and ER-2 measurements in the lower stratosphere, e.g., Figure 6a) can be combined to produce the schematic of the global Γ distribution shown in Figure 7. As it is based almost exclusively on Northern Hemisphere data (see Table 1), the schematic is hemispherically symmetric. The few available Southern Hemisphere data, as well as model simulations, indicate slightly greater values of Γ in the Southern Hemisphere (e.g., Figure 6a and Figure 7 of *Andrews et al.* [2001b]). Also, because of the limited temporal coverage the sche-

matic represents the annual mean Γ. Available data and models suggest larger seasonal variations at high latitudes than at low latitudes.

[38] Despite these qualifications the general shape of the isopleths in Figure 7 is probably realistic and illustrates distinctive features about mean age. The isopleths are similar to those of other chemically active long-lived tracers, such as N_2O, CH_4, and CFCs, in that they bulge upward in the tropics and slope down to high latitudes. As with all long-lived tracers, the shape of isopleths of mean age are determined by the balance of the meridional mass (Brewer-Dobson) circulation, which tends to increase latitudinal slopes, and isentropic mixing, which tends to decrease the slopes [e.g., *Plumb and Ko*, 1992] (see Figure 1). However, the near-vertical isopleth orientations for mean age (all balloon observations in middle latitudes show near-zero vertical gradients in age above around 25 km) are not seen in chemically active long-lived tracers, which have vertical gradients in their mixing ratio because they undergo photochemical processes in the middle and upper stratosphere.

[39] Despite the weakness of the vertical gradients in certain regions, mean age increases monotonically with height throughout the stratosphere, a fact which at first sight may seem surprising. Transport by the advective residual mean circulation alone would lead to the highest ages in the polar lower stratosphere, whose parcels would have descended from the highest altitudes following ascent in the tropics [e.g., *Rosenlof*, 1995]. However, because of wave-driven mixing, there is a broad distribution of transit times throughout the extratropics, and isolated descent over multiyear timescales is prevented.

3.2. Impact of Chemical Losses

[40] As discussed in section 2.3, estimates of Γ from the time lag in tracer concentrations are sensitive to chemical loss processes. For tracers with only mesospheric loss we expect the effect to be largest in the mesosphere and inside the stratospheric polar vortices [*Hall and Waugh*, 1998]. It is therefore possible that discrepancies in estimates of Γ in these regions from different tracers could be due to chemical losses in one of the tracers.

[41] Although SF_6 has a long global lifetime, descent of air from the mesosphere (where the ultimate chemical destruction of SF_6 occurs [*Ravishankara et al.*, 1993]) into the polar vortices may have an appreciable impact on mean age estimates, because the mean age heavily weights the tail region of the age spectrum. As mentioned in section 3.1, several sets of simultaneous CO_2 and SF_6 measurements in vortex air show larger Γ from SF_6 than from CO_2. Three different platforms made SF_6 and CO_2 measurements in vortex fragments in June 1997, and all show Γ from SF_6 ~2 years older than Γ from CO_2 (e.g., Figure 6d) [*Strunk et al.*, 2000]. Furthermore, more recent measurements inside the 1999/2000 Arctic vortex also show Γ from SF_6 larger than that from CO_2 (with the bias increasing with altitude) (J. Elkins and A. Andrews, personal communication, 2000), and CO measurements inside the vortex and model calculations indicate that mesospheric air had descended down to the lower stratospheric vortex [*Plumb et al.*, 2002]. This supports the hypothesis that the difference between SF_6 and CO_2 estimates of Γ in the vortices is primarily due to influence of mesospheric depletion of SF_6. (Note that although photolytic conversion of CO_2 to CO occurs in the mesosphere, this corresponds to an overestimation in Γ from CO_2 of less than a month.) Quantification of the mesospheric depletion of SF_6 and impact on Γ from SF_6 is difficult because of the large uncertainty in the processes involved and the reaction rates [*Reddman et al.*, 2001].

[42] The influence of mesospheric air depleted in SF_6 may also explain the inconsistency between the values of Γ = 8–10 years from SF_6 at 30 km inside the vortex [*Harnisch et al.*, 1996] and the younger values of 5–6 years inferred from measurements of chlorine and fluorine families at 55 km [*Zander et al.*, 1996, *Russell et al.*, 1996; *Anderson et al.*, 2000]. Note also that the maximum Γ from CO_2 measurements is around 6 years. These younger ages from several tracers are hard to reconcile with the high SF_6 values without an SF_6 chemical bias. However, a further complication is the good agreement between Γ from CF_4 and SF_6 [*Harnisch et al.*, 1999]. As the global lifetime of CF_4 is thought to be much greater than even SF_6 [*Ravishankara et al.*, 1993], one would expect that if losses are affecting SF_6, then Γ from SF_6 would be greater than that inferred from CF_4. Note also that measurements of CF_4 around 60 km indicate Γ around 12 years [*Harnisch et al.*, 1999], twice the values inferred from the measurements of chlorine and fluoride families.

3.3. Interannual Variations in Mean Age

[43] Increasing attention has been focused on long-term changes in stratospheric circulation as a part of climate change. Modeling work suggests that the stratospheric circulation may respond appreciably to increasing greenhouse gases [*Shindell et al.*, 1998], and trace gas measurements from the HALOE instrument show low-frequency variability that may be caused by circulation changes [*Nedoluha et al.*, 1998; *Randel et al.*, 1999]. In principle, mean age can be used to isolate changes in trace gas distributions due to changes in circulation. Unfortunately, different tracers, instruments, and platforms have different degrees of uncertainty, making it difficult to construct reliable time series from the various mean age estimates. However, there are a few studies which have reported mean age measurements over a number of years using the same tracer measurement technique.

[44] *Schmidt and Khedim* [1991] analyzed balloon whole air samples of CO_2 over Europe from 1976 to 1990, *Nakazawa et al.* [1995] analyzed similar measurements over Japan from 1985 to 1991, and *Boering et al.* [1996] and *Andrews et al.* [2001b] analyzed in situ aircraft

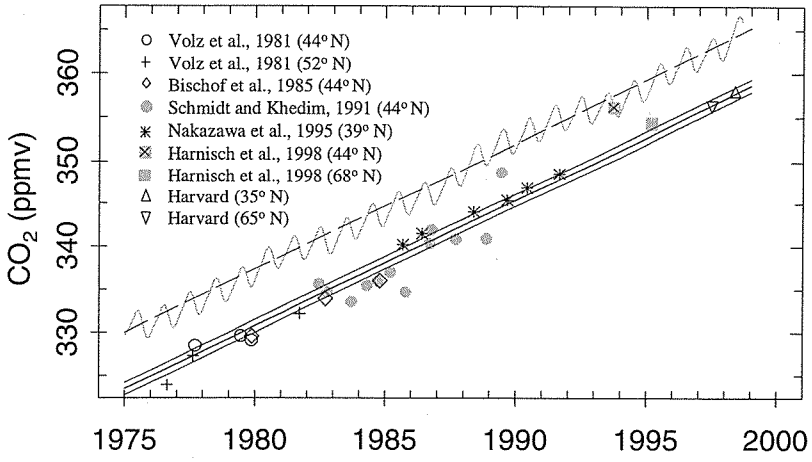

Figure 8. Variation of observed stratospheric CO_2 with time for balloon measurements in Northern Hemisphere middle latitudes. Symbols correspond to average values in the region above 20–25 km where there are weak vertical gradients (see legend for references). The shaded curve represents the stratospheric boundary condition for CO_2, and the long-dashed curve is a linear fit to this boundary condition. The bold solid curve is this fit delayed by 4.5 years, and the thin curves correspond to delays of 4 and 5 years (From *Andrews et al.* [2001b].)

and balloon CO_2 measurements from 1992 to 1999. Figure 8 shows the CO_2 balloon data from these studies, as well as those of *Bischof et al.* [1985] and *Harnisch et al.* [1988]. The data points represent averages over the midlatitude regions above roughly 25 km where mean age (and CO_2) varies little with height. Although the *Schmidt and Khedim* [1991] data show large interannual variations with a time period of 3–5 years (which corresponds to Γ varying by as much as 4 years within a 2-year period), the other data sets show near-linear increases in stratospheric CO_2 and therefore little interannual variation in Γ. This includes the *Nakazawa et al.* [1995] data, which overlaps the *Schmidt and Khedim* [1991] period (1985–1990). Note that the data of *Harnisch et al.* [1998] appear to be outliers. As discussed in section 3.2, it has been argued that these data may have been affected by contamination.

[45] A further multiyear data set of Γ can be obtained from estimates of total chlorine Cl_{tot} and fluorine F_{tot} from Halogen Occultation Experiment (HALOE) measurements of upper stratosphere HCl and HF (in the upper stratosphere HCl and HF make up the vast majority of Cl_{tot} and F_{tot}, respectively) [e.g., *Anderson et al.*, 2000]. Although there is large uncertainty in the stratospheric mean age estimates from these data, there is no sign of large interannual variability. Therefore, except for the *Schmidt and Khedim* [1991] analysis, there is no evidence for large interannual variation of Γ over timescales of several years. Longer time series will help to establish the variability more precisely.

[46] The above multiyear data sets apply to middle and high latitudes. At present the only tropical data are from the few vertical balloon profiles of SF_6 and CO_2 as part of the OMS campaign [*Andrews et al.*, 2001b; *Ray et al.*, 1999], all of which occurred in February and November 1997. Thus the magnitude of interannual variation in Γ within the tropics is unknown. As there is large interannual variability of winds in the tropics, due primarily to the quasi-biennial oscillation (QBO), we expect there to be some interannual variability in Γ. In fact, recent modeling studies using analyzed winds from 1992 to 1997 show interannual variations in Γ which are correlated with the QBO (W. Norton, personal communication, 1999).

3.4. Phase Lag Times

[47] As discussed in section 2, a second class of timescales, phase lag times τ_ω, can be defined from conserved tracers whose mixing ratios at the tropical tropopause vary periodically. Two tracers with dominant annual cycles that have been used to estimate τ_ω for an annual cycle are carbon dioxide CO_2 [*Boering et al.*, 1994, 1995, 1996; *Andrews et al.*, 1999] and total hydrogen $\hat{H} = H_2O + 2CH_4$ [*Mote et al.*, 1996, 1998; *Weinstock et al.*, 2001]. The annual cycle in stratospheric CO_2 is forced by the annual cycle in surface CO_2, the result of seasonal variations in biota sources and sinks, whereas the cycle in $\hat{H}$ is forced by the annual cycle in tropical tropopause temperatures, which regulate (via dehydration) the values of H_2O (and $\hat{H}$) entering the stratosphere.

[48] Figure 9a shows several observational estimates of the vertical variation in the tropical stratosphere of τ_ω for an annual cycle. The squares correspond to τ_ω determined from 4 years of measurements of H_2O and CH_4 from the HALOE instrument on UARS based on an empirical orthogonal function analysis by *Mote et al.* [1998], the solid triangles correspond to τ_ω from in situ measurements of H_2O and CH_4 (H. Vomel, Personal communication, 2000), and the solid circles correspond to τ_ω from in situ measurements of CO_2 from the ER-2

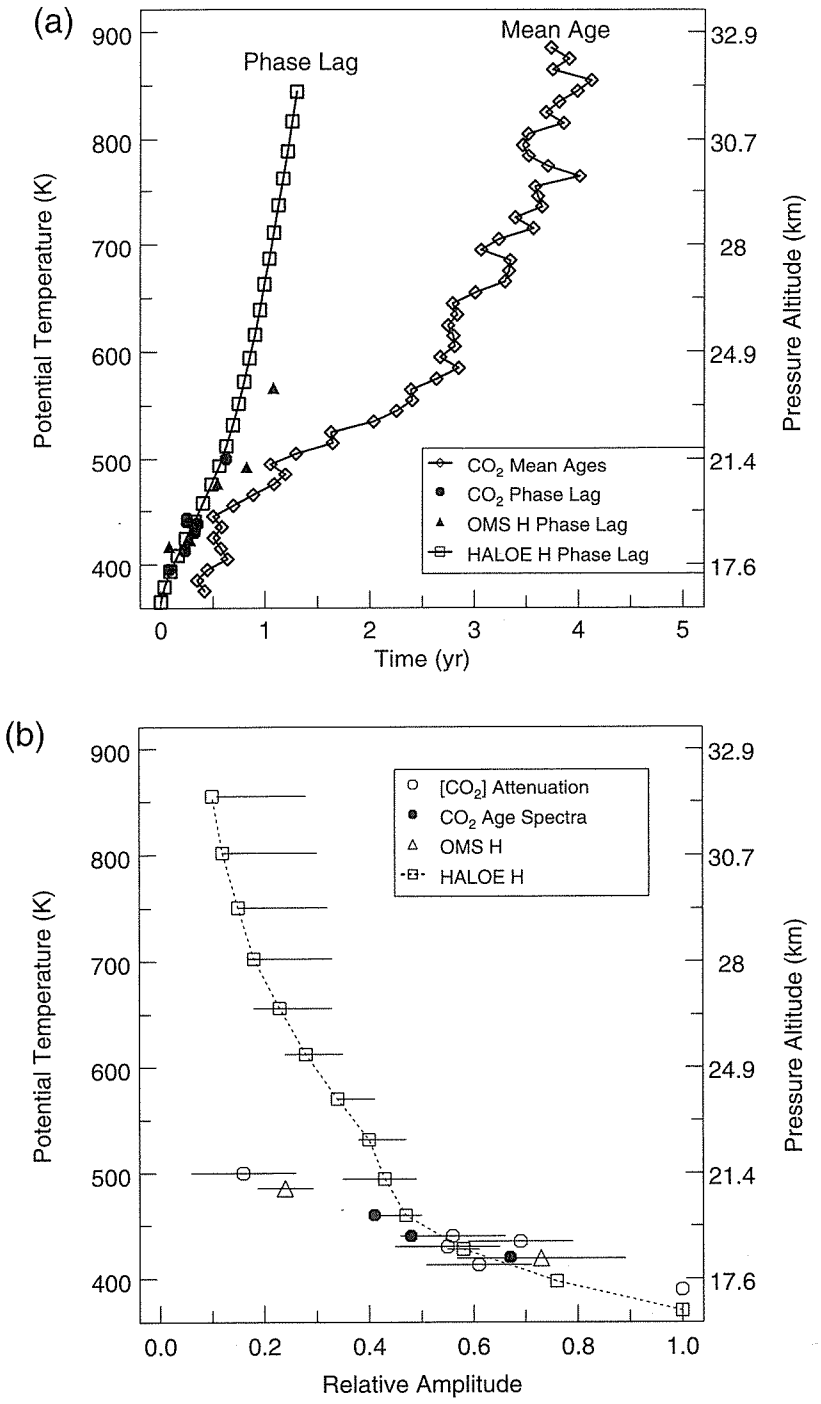

Figure 9. (a) Observational estimates of the vertical variation in the tropical stratosphere of τ_ω for an annual cycle. Squares correspond to τ_ω determined from 4 years of measurements of H_2O and CH_4 from the Halogen Occultation Experiment (HALOE) [*Mote et al.*, 1998], the solid triangles correspond to τ_ω from in situ measurements of H_2O and CH_4 (H. Vomel, personal communication, 2000), and the solid circles correspond to τ_ω from in situ measurements of CO_2 from the ER-2 aircraft [*Andrews et al.*, 1999]. Also shown are estimates of Γ from balloon measurements of CO_2. (b) Observed amplitude as a fraction of the tropopause value from HALOE measurements of $\hat{H}$ and from in situ aircraft and balloon measurements of CO_2 and $\hat{H}$ models. (Adapted from *Park et al.* [1999].)

aircraft [*Andrews et al.*, 1999]. See *Park et al.* [1999] for more details on the calculations of τ_ω. Overall, the agreement between the different estimates of τ_ω is very good. The values of τ_ω shown are approximately equal to the timescale for tropical upwelling; for example, assuming constant upwelling, $\tau_\omega(26\text{ km}) - \tau_\omega(16\text{ km}) = 1$ year corresponds to an average ascent rate of 0.3 mm/s. Note that the values plotted in Figure 9a represent annual

averaged τ_ω, but the observations show a seasonal variation in τ_ω [*Mote et al.*, 1996; *Boering et al.*, 1996; *Andrews et al.*, 1999], with younger values in northern winter. This seasonal variation is consistent with the seasonal variation in the residual circulation, in which there is a stronger tropical upwelling during northern winter [e.g., *Holton et al.*, 1995].

[49] Also shown in Figure 9a are estimates of Γ from balloon measurements of CO_2 [*Andrews et al.*, 2001b] (simultaneous measurements of SF_6 yield similar ages; see Figure 6b). It can clearly be seen that $\Gamma > \tau_\omega$, with large differences in the middle stratosphere. This is consistent with theory and models: As discussed in section 2, the mean age weights the long tails of the age spectra heavily. For an annually periodic signal the tail region is averaged out, and τ_ω is biased toward the peak in the spectra and is younger than Γ. Physically, old air from the extratropics is mixed into the tropics, greatly increasing the tropical mean age. However, this extratropical air contains components with phases from several full annual cycles of CO_2 or H_2O at comparable magnitude, which therefore roughly cancel and contribute little to the phase of the tropical air.

[50] The amplitude of annual cycles also provides valuable information on stratospheric transport, in particular tropical-midlatitude mixing. Figure 9b shows the observed amplitude as a fraction of the tropopause value from HALOE measurements of $\hat{H}$ and from in situ aircraft and balloon measurements of CO_2 and $\hat{H}$. The agreement between the different observations is less good than for the phase lag times, with the in situ balloon measurements indicating more rapid attenuation than the satellite measurements. There are potential sources of error in the estimates of amplitude from both measurements. The HALOE likely underestimates the peak-to-peak amplitude near the tropopause because of coarse vertical resolution [*Mote et al.*, 1996]. On the other hand, the in situ measurements are derived from only a few balloon flights at a single latitude (7°S) and therefore may not represent a tropical climatological profile. In fact, *Jost et al.* [1998] observed abrupt signatures of filaments of entraining extratropical air in this region. Nonetheless, even with this uncertainty, the observational estimates are useful in evaluating models, as discussed in section 4.2.

[51] The phase and amplitude of the annual cycle and the mean age have different sensitivities to tropical transport rates. This has allowed them to be used in combination to estimate simultaneously ascent rates, mixing rates with the extratropics, and vertical diffusion within the tropics. *Hall and Waugh* [1997b] fit mean age and annual cycle solutions of a 1-D diffusive-advective-entraining model with constant coefficients to deduce these rates. *Mote et al.* [1998] used a similar analysis but allowed for vertical variation in the transport coefficients and used CH_4 instead of mean age. The resulting rate estimates were similar, when the results of *Mote et al.* [1998] are averaged over the the domain of *Hall and Waugh* [1997b] (16–32 km). *Mote et al.* [1998], however, deduced a region from ~20 to 24 km of high tropical isolation, reflecting the observation that over this region the HALOE H_2O annual cycle amplitude attenuates very little. Overall, these analyses result in the attractive and straightforward interpretation of the annual cycle signal: The phase speed approximately equals the upwelling rate, and the fractional attenuation approximately equals the fraction of tropical air with extratropical origin.

[52] The phase lag time of an annual cycle increases with latitude from the tropics. *Boering et al.* [1994] reported simultaneous in situ measurements of CO_2 and N_2O and deduced from the compactness of the tracer-tracer scatterplot that in the lower stratosphere the CO_2 annual cycle must propagate from the tropics to midlatitudes in no more than several weeks. This timescale, however, must be interpreted with caution. Transport to the lower midlatitude stratosphere occurs by a variety of pathways with a range of transit times. Model studies suggest this range is well over a year, so that all phases of the tropical tropopause annual cycle are present in midlatitude parcels. The resulting phase cancellation leaves a small midlatitude amplitude with a residual phase whose lag from the tropopause is much less than the mean age. In other words, while the phase lag is several weeks, the time to move, for example, half the tropical air to midlatitudes is significantly longer. However, as discussed in section 3.5, *Andrews et al.* [2001a] have argued recently that midlatitude lower stratospheric air may be composed of distinct young and old components and that the phase lag time is a direct measure of the young component.

3.5. Estimates of the Age Spectra

[53] The mean age and phase lag time are pieces of information about the full age spectrum. The age spectra themselves cannot be measured directly, but recently indirect estimates of the spectra have been made from observations.

[54] *Andrews et al.* [1999] calculated empirical age spectra from the time series of in situ CO_2 measurements in the tropical lower stratosphere, assuming that the spectra have the same functional form as the spectra for the 1-D model (equation (8)). They obtained the best fit to the data with seasonally varying spectra in which both Γ and τ_M (modal time) are younger in northern winter. From the derived spectra, *Andrews et al.* [1999] calculated the phase lag time and attenuation of an annually repeating tracer (see Figure 9) and also generated vertical profiles of H_2O which agree well with in situ observations.

[55] *Andrews et al.* [2001a] have recently extended this type of analysis to midlatitudes and find a better fit to the CO_2 data using a bimodal age spectrum. They interpreted the younger, narrow peak as representing rapid quasi-horizontal wave mixing and the older, broader peak as representing "up-and-over" transport via the

mean meridional circulation. One way such bimodality can occur is if a region of relatively slow outflow from the tropics to extratropics sits above a region of more rapid outflow. This is consistent with the analysis of *Mote et al.* [1998]. These authors inferred from satellite $\hat{H}$ observations that over the region 20- to 24-km region the tropical upwelling rate increases with height, so that, by continuity, the outflow is reduced. Two-way exchange was also seen to be strongly inhibited over this region.

[56] In a different approach, *Johnson et al.* [1999] have used Fourier analysis and singular value decomposition to deconvolve the time-mean age spectrum from the $\hat{H}$ time series reconstructed from balloon and satellite measurements. This approach makes no assumptions about a functional form. Although the resulting tropical age spectra are noisy, the modal time clearly increases with height. In fact, the increase in modal time of 1.6 years from 16.5 to 31.5 km implies a mean velocity of 0.3 mm/s in close agreement with independent estimates of the tropical upwelling [*Rosenlof*, 1995; *Eluszkiewicz et al.*, 1996]. The agreement corroborates the close association of the modal time and the timescale for vertical advective ascent, confirming that mixing plays at most a small role in tropical vertical transport.

[57] As discussed in section 2.3, the decay rate of the age spectrum for long transit times corresponds to the *e*-folding time of the longest-lived mode of stratospheric transport. An observational estimate of this timescale has recently been made by *Ehhalt et al.* [2002]. They analyzed measurements of the tritium content in stratospheric water made between 1975 and 1983 and found little vertical variation but a strong decay with time. After taking account of radioactive decay and increases in stratospheric water, they calculated a timescale of 7.7 years for transport out of the stratosphere. Interpreting this as the *e*-folding time of the longest-lived mode, this timescale then constrains the tail of the age spectra and also provides an additional test on model transport.

3.6. Summary

[58] The mean age Γ can be estimated from measurements of several different chemical species and families (e.g., CO_2, SF_6, and total chlorine). There is good agreement among the various estimates, except for SF_6 in the polar vortex where mesospheric depletion of SF_6 likely causes an overestimate of Γ. In the lower stratosphere (20 km), Γ is ~1 year at the equator and increases to 4–5 years at high latitudes, with the largest latitudinal gradients in the subtropics. At all latitudes, Γ generally increases with height, attaining values of ~4 years at 30 km in the tropics and 6 years at high latitudes. Above about 25 km, however, vertical gradients are weak in midlatitudes. Balloon measurements of CO_2 in northern middle and high latitudes indicate that Γ has changed little over the past 25 years.

[59] The propagation of an annually periodic tracer signal has been characterized from tropical balloon and satellite measurements of CO_2 and total hydrogen ($H_2O + 2CH_4$). The phase lag time τ_ω is significantly smaller than the mean age (at 30 km, $\tau_\omega \approx 1$ year compared to $\Gamma \approx 4$ years) and is approximately equal to the timescale for tropical advective upwelling (≈ 0.3 mm/s).

[60] Although age spectra cannot be measured, several indirect estimates have been made from observations of CO_2 or H_2O. The most recent and detailed analysis indicates that spectra in the extratropical lower stratosphere are bimodal with a narrow, young peak (representing rapid quasi-horizontal wave mixing) and a broad, older peak (representing "up-and-over" transport via the mean meridional circulation).

4. MODELS

[61] Transport timescales derived from tracers are independent of photochemistry and are therefore excellent diagnostics for evaluating model transport. In this section we discuss model simulations of the mean age and the phase lag time and amplitude of periodic tracers.

4.1. Mean Age Simulations

[62] There are several ways to calculate mean age in a model stratosphere. The stratospheric response to an impulsive mixing ratio boundary condition (approximating a delta function) at the surface yields the age spectrum, and the mean age is the first moment, as in equation (4). In the presence of annual and interannual transport variations one needs to simulate a series of delta functions each centered on a successive date to obtain the full time-varying age spectrum (function of transit time and date) and mean age (function of date). This is computationally intensive, as it requires many tracers. In practice, a single delta function yields a good approximation to the annually averaged age spectrum and mean age. A second way to compute mean age is to simulate the response to a linearly increasing mixing ratio boundary condition [*Hall and Prather*, 1993]. In steady (or cyclostationary) state the whole atmosphere is increasing at the same rate, and the mean age is the lag time at stratospheric points from the troposphere. This technique has the advantage of requiring only a single tracer to obtain the full time-varying mean age. A third technique for the mean age is to obtain the steady state response to a tracer with unit source for mixing ratio uniformly distributed over the whole stratosphere and a zero tropospheric boundary condition. This is summarized in equation (9), has been employed by *Neu and Plumb* [1999] in the stratosphere, and is the most common technique in ocean tracer studies [e.g., *Thiele and Sarmiento*, 1990; *England*, 1995].

[63] The agreement between mean age computed as the first moment of a single delta function response and as computed from the linear tracer time lag is close, when considered as an annual mean [see *Hall et al.*, 1999, Figure 3]. Moreover, both agree with the time lag

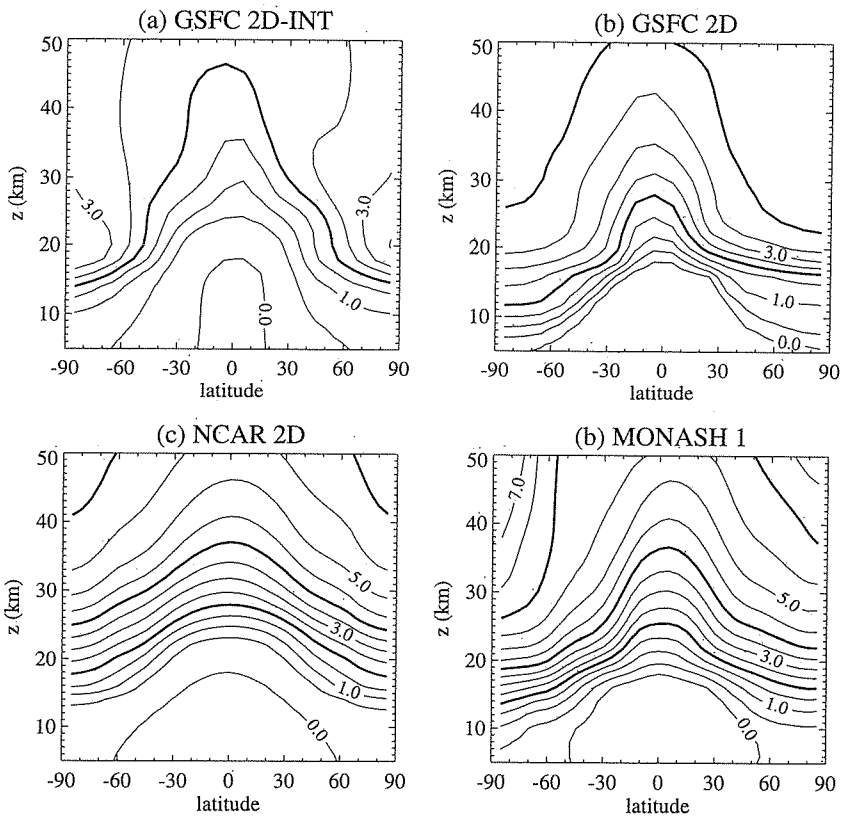

Figure 10. Annual mean zonal-mean Γ distributions from the (a) Goddard Space Flight Center (GSFC) 2D-INT [*Rosenfield et al.*, 1997], (b) GSFC 2D [*Fleming et al.*, 1999], (c) NCAR2D [*Park et al.*, 1999], and (d) MONASH1 [*Waugh et al.*, 1997] models. Contour intervals are 0.5 year, and the bold contours indicate 2-year intervals. (Adapted from *Hall et al.* [1999].)

obtained from direct simulations of SF_6 or CO_2, including realistic surface-distributed and temporally varying sources. This indicates that the stratospheric mean age is robust; that is, it is not sensitive to the tropospheric details of the tracer.

[64] Mean age has been calculated by one or more of these methods within a large number of 2-D and 3-D models. The more than 20 models that participated in MM2 contributed mean age simulations and had these simulations compared to observations [*Park et al.*, 1999; *Hall et al.*, 1999]. A number of other models that did not participate in MM2 have also simulated mean age [e.g., *Bacmeister et al.*, 1998; *Manzini and Feichter*, 1999; *Eluskiewicz et al.*, 2000; *Reddmann et al.*, 2001; *Zhu et al.*, 2000]. Comparison of Γ among different models, four of which are included in Figure 10, shows large differences. The differences between these four models are representative of the differences between all models in the MM2 study (see *Hall et al.* [1999, Figures 6 and 7] for the mean age distributions of the individual MM2 models). There is a large variation in the simulated magnitudes: at 50 km in the tropics the mean age varies from around 2 years to 5.5 years. There are also large differences in the shape of the Γ isopleths. In some models the mean age has a local maximum in the high latitude lower stratosphere (e.g., Figure 10a), while in others the mean age increases monotonically throughout the stratosphere and mesosphere (e.g., Figures 10b–10d). In some models, mean age contours bulge up sharply in the tropics (e.g., Figures 10b and 10d), while in others the tropical region is less distinct (e.g.,Figures 10a and 10c). These differences reflect and diagnose differences in the transport between the models.

4.2. Comparison with Observations

[65] The observations discussed in section 3.1 can be used to evaluate the mean age, and hence the transport, within models. As discussed in section 4.1, there are qualitative differences in the shape of Γ isopleths from different models. Comparisons with the schematic Γ distribution based on observations shown in Figure 7 indicate that the models that produce a Γ distribution with maximum age (of around 6 years) in the upper levels of the model and steep meridional gradients in the subtropics are most realistic.

[66] A direct and quantitative comparison of mean age from MM2 models and CO_2 and SF_6 observations is shown in Figure 6. Blue-shaded regions represent the ranges of mean age simulated by a majority of the MM2 models, while the blue curves represent other selected MM2 models. The red curves and symbols show the observed mean age (see Figure 6 caption for details).

[67] Figure 6 illustrates further the large spread in the model mean ages seen in Figure 10 and shows the unrealistic features of mean age in many models: (1) Most models underestimate the magnitude of mean age; (2) most models do not reproduce the steep latitudinal gradients in the subtropical lower stratosphere; (3) several models exhibit a lower stratospheric Γ maximum at middle and high latitudes, which is not observed. (The lower stratosphere mean age spikes in the OMS profiles shown in Figure 6d are due to sampling through remnants of old polar vortex air and would not survive annual averaging.) These model-data differences indicate that most models have significant inaccuracies in their transport.

[68] As discussed in section 3.5, *Ehhalt et al.* [2002] obtained a value of $\tau_0 = 7.7$ years for the e-folding time of the longest-lived mode of stratospheric transport from measurements of the tritium content of stratospheric water. This value is larger than the value for the models in the MM2 study, where $\tau_0 < 4$ years for nearly all models. This implies that the model age spectra decay too rapidly, which is consistent with the underestimation of the mean age by models.

4.3. Sensitivity to Aspects of Circulation

[69] Mean age is a measure of aggregate transport, determined by the complex interplay of advection and diffusion on all scales. To better understand why there is such a large variation in Γ among models, it helps to analyze the sensitivity to specific aspects of the circulation.

[70] The strength of the Brewer-Dobson circulation has a large impact on the magnitude of Γ (with a slower circulation resulting in older air), but it has much less impact on the shape of the Γ isopleths, as has been demonstrated in the 2-D studies of *Bacmeister et al.* [1998] and *Li and Waugh* [1999]. This is also well illustrated by comparing simulations using the same off-line transport model driven by winds archived from two different versions of the NCAR MACCM2 model [*Boville*, 1995] (referred to as the MONASH1 and MONASH2 models in the MM2 study [*Hall et al.*, 1999]). The two MACCM2 versions differed in their gravity wave parameterized sources: The later version (MONASH2) included additional parameterized sources which alleviated the strong cold pole bias of the earlier version (MONASH1) and significantly increased the residual circulation magnitude. Consistent with the 2-D model sensitivity studies, the version with stronger circulation has younger air (by ~25%) but similarly shaped Γ isopleths.

[71] In contrast, the quasi-horizontal mixing rate in the extratropics has limited effect on the magnitude but can have a large impact on the shape of the Γ isopleths. Decreased mixing leads to steeper slope of subtropical Γ isopleths, which can be seen directly for MM2 2-D models by comparing their Γ distributions and horizontal diffusivities [*Hall et al.*, 1999, Figures 6 and 10]. In fact, if extratropical mixing is weak enough, the Γ has a local maximum in the polar lower stratosphere. Mean age in such a model is much like the advection time by the residual circulation, as seen both in models [*Bacmeister et al.*, 1998; *Hall et al.*, 1999; *Yudin et al.*, 2000, *Li and Waugh*, 1999] and from trajectory calculations driven by an observationally based residual circulation [*Rosenlof*, 1995]. However, observations show that mean age does not exhibit a lower stratospheric maximum (except when isolated vortex fragments are encountered) but rather increases monotonically with height at all latitudes, albeit weakly in the midlatitude middle stratosphere. Models exhibiting such a Γ maximum likely have too little quasi-horizontal mixing in the extratropics. Notably, all 2-D MM2 models that calculate the horizontal diffusivities interactively using a wave-breaking parameterization, as given by *Garcia et al.* [1992], display this unrealistic lower stratospheric maximum in Γ.

[72] Many of the sensitivities of mean age to large-scale circulation features can be understood with the idealized tropical leaky pipe model of stratospheric transport [*Plumb*, 1996; *Neu and Plumb*, 1999] described in section 2.2. *Neu and Plumb* [1999] solved for mean age in this model, revealing the inverse relationship between mean age and residual circulation magnitude seen in the 2-D and 3-D models. In addition, the mean age was found to increase with increased tropical-midlatitude mixing due to enhanced recirculation of stratospheric air. *Neu and Plumb* [1999] also obtained the counterintuitive result that the mean age gradient across the tropical barrier is only weakly sensitive to tropical-midlatitude mixing. With increased mixing the mean age isopleths "flatten," but the apparent decrease in horizontal gradient is approximately compensated by the overall increase in mean age magnitude.

[73] In addition to large-scale circulation features, the mean age is sensitive to the numerical transport scheme, as illustrated in a recent study by *Eluszkiewicz et al.* [2000]. They simulated Γ within the Geophysical Fluid Dynamics Laboratory SKYHI GCM using several different transport schemes: two centered finite difference schemes, the semi-Lagrangian scheme of *Rasch and Williamson* [1990], and the mass-conserving flux form semi-Lagrangian schemes of *Lin and Rood* [1996]. In addition, *Eluszkiewicz et al.* [2000] used particle trajectories (employing both sigma and potential temperature as vertical coordinates) driven by the SKYHI winds to obtain mean age. The mean age distribution varied widely with advection scheme, ranging from as old as 10 years in the upper stratosphere for one of the centered difference schemes to ages everywhere younger than 3 years for the semi-Lagrangian scheme. Moreover, the semi-Lagrangian calculation displayed a high-latitude lower-stratosphere mean age maxima not seen using the other schemes.

[74] It is important to note, however, that other comparisons of models using the same circulation fields but

different advection schemes show much less sensitivity than reported by *Eluszkiewicz et al.* [2000]. For example, the mean age distributions of two 3-D off-line transport models (MONASH2 and GMI-NCAR) in the MM2 study that employed the same meteorological data from the NCAR MACCM2 model but used the different advection schemes (the two semi-Lagrangian advection schemes considered by *Eluszkiewicz et al.* [2000]) are very similar [*Hall et al.*, 1999]. Similarly, the UCI23 and GMI-GISS models in the MM2 study use the same meteorological data (the GISS middle atmosphere GCM) but different advection schemes (flux form semi-Lagrangian for GMI-GISS and quadratic upstream [*Prather*, 1986] for UCI23) and produce very similar Γ distributions. The insensitivity of these Γ simulations to the advection scheme shows that the differences between some model simulations are due to the circulation fields and not the advection schemes.

[75] More recently, *Mahowald et al.* [2002] compared age simulations from two versions of an off-line model using meteorological data from the NCAR MACCM2 model, one using a standard hybrid pressure vertical coordinate and the other using a new hybrid isentropic coordinate. The simulations using the isentropic coordinate agreed better with observations, and they argued that the improved simulation was due to reduced numerical vertical diffusion.

[76] These model analyses indicate that some caution is required when interpreting simulated mean age solely in terms of the large-scale circulation fields and that the vertical coordinate and advection scheme (as well as other characteristics of the transport scheme) may both contribute to the problems with mean age simulations.

4.4. Propagation of Annually Repeating Tracers

[77] The propagation into the stratosphere of the annually periodic tracer signals in $\hat{H}$ and CO_2 complement mean age as tests of model transport. For this reason, annually periodic tracer signals were employed in the MM2 study and have been used in other model studies as well. Figure 11 shows phase lag time τ_ω and the peak-to-peak amplitude A_ω as functions of height in the tropical stratosphere for the MM2 model participants, as well as the observations discussed in section 3.4. Most MM2 models propagate the annual signal too rapidly in the vertical. Average phase speeds over the 16- to 26-km region ($\Delta z/\Delta\tau_\omega$) range from 0.30 to 1.09 mm/s [*Hall et al.*, 1999], whereas the HALOE taperecorder average speed is ~0.3 mm/s [*Mote et al.*, 1998]. The amplitude of the models is more difficult to evaluate, since the observational estimates of its height variation show considerable spread. However, if one considers the attenuation following an upwelling seasonal impulse over a year (rather than attenuation over a fixed height range), then the observational and model spreads are reduced and are sufficiently separated to show that most MM2 models overattenuate the signal [*Hall et al.*, 1999].

[78] The overattenuation of A_ω by models at first sight could be due to either too much mixing of tropical and extratropical air or too much vertical diffusion (numerical or explicit) within the tropics. The 1-D advective-diffusive-entraining observational analyses [*Hall and Waugh*, 1997b; *Mote et al.*, 1998] described in section 3.4 separate the roles of these processes and obtain from 100-hPa and 10-hPa dilution timescales between 1 and 1.5 years (with narrow regions of much slower mixing) and diffusivities well under 0.1 m^2/s. In this regime, diffusion plays little role in propagating the signal. Several 2-D MM2 models had explicit vertical diffusivities significantly larger than 0.1 m^2/s. *Fleming et al.* [1999] confirmed that low diffusivities are more realistic by performing sensitivity experiments with the Goddard Space Flight Center 2D model and finding convergence of Γ to realistic profiles for values of K_{zz} less than 0.1 m^2/s.

4.5. Summary

[79] The mean age and the phase and amplitude of annually periodic tracers represent stringent tests of transport in stratospheric models. These quantities have been simulated by a large number of two- and three-dimensional chemical transport models, and the simulated fields have been intercompared and compared with observations. There is a wide variation among models in both the magnitude and spatial structure of the mean age and annual cycle phase, and when compared with observations, several unrealistic features can be seen in most models. Such discrepancies with observations indicate that most stratospheric models have significant inaccuracies in their transport. The causes of the deficiencies vary from model to model. Both the large-scale circulation and numerics, including the nature of the vertical coordinate and the advection algorithm, play a role in determining the mean age and characteristics of the annual cycle propagation.

5. RELATIONSHIPS BETWEEN MEAN AGE AND OTHER TRACERS

[80] Mean age is a pure transport diagnostic. Modelers are ultimately interested in simulating accurately the distribution of trace gases that are affected by both transport and photochemistry. It is therefore important to determine the extent to which constraints imposed by mean age observations are relevant for the distributions of various reactive gases.

[81] There are significant model-to-model variations in simulations of long-lived photochemically active trace gases such as N_2O, NO_y, and Cl_y, and these variations are similar in many respects to those of mean age. Figure 12 shows the annual mean, zonal-mean N_2O for the models shown in Figure 10. Comparison of Figures 10 and 12 shows that the isopleths of Γ and N_2O are almost parallel in middle and low latitudes, and models with strong (weak) subtropical meridional gradients in Γ also

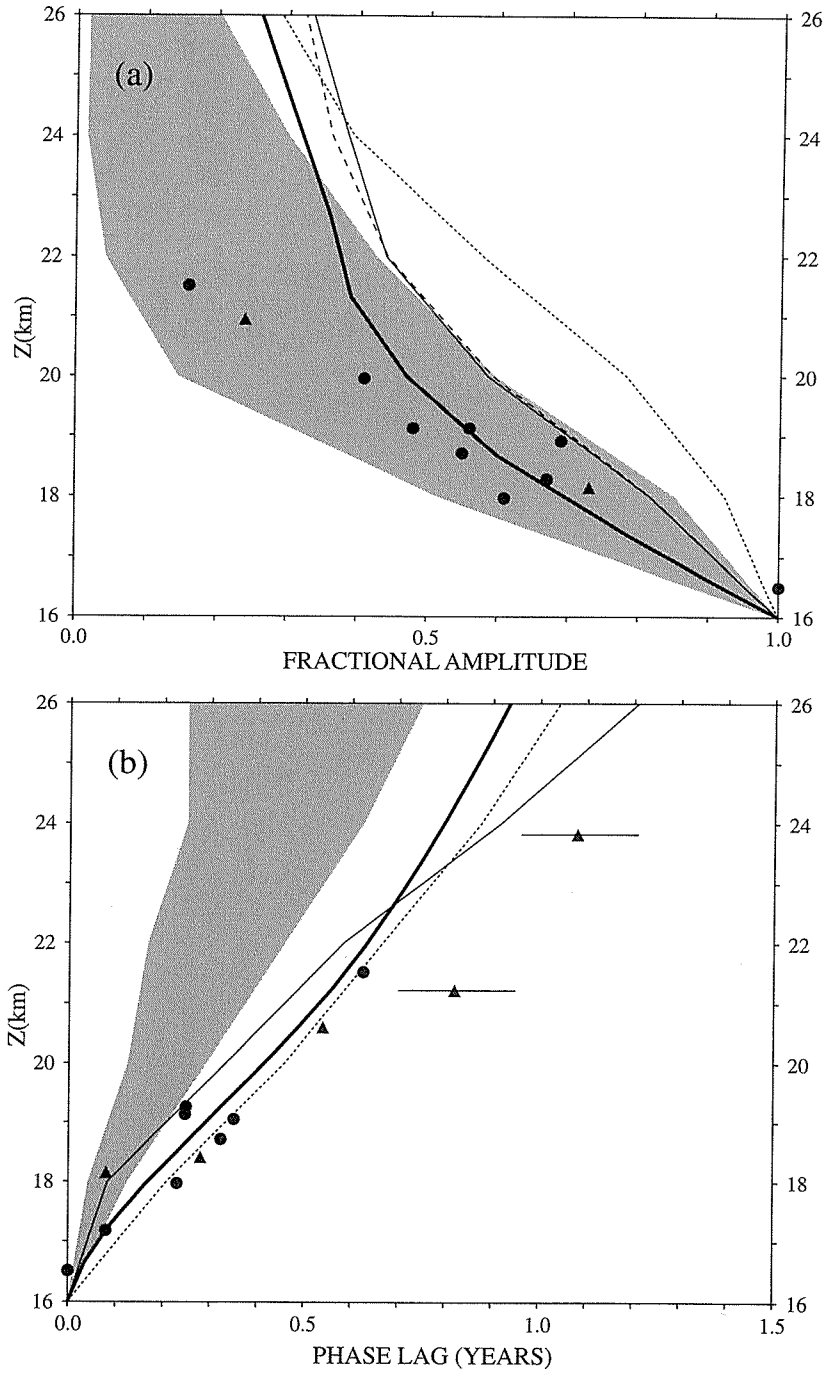

Figure 11. Equatorial profiles of (a) $A_\omega(z)$ and (b) $\tau_\omega(z)$ for a range of models and observations. All amplitudes are normalized to unity, and the phase lag is taken as zero at 16 km. The shaded region indicates the range of most models in the MM2 study, while the individual (thin) lines respresent several models falling outside the range. The bold solid line represents the analysis of HALOE $\hat{H}$ [*Mote et al.*, 1998], and the symbols represent analysis of in situ measurements of CO_2 (circles) and $\hat{H}$ (triangles). The error bars on the top two in situ phase lag points are estimated from the uncertainity in the tropopause $\hat{H}$ time series. (From *Hall et al.* [1999].)

have strong (weak) N_2O gradients. Also, models with younger (older) Γ generally have higher (lower) N_2O. Variations in lower stratospheric N_2O, NO_y, and Cl_y across the set of MM2 models are well correlated with the corresponding variations in Γ (see tracer-tracer scatterplots in Figure 15 of *Hall et al.* [1999]). This close relationship indicates that inaccuracies in the model transport, as revealed by the mean age, have a large impact on simulations of chemically active tracers. Transport inaccuracies may be the principal source of uncertainty in simulations of the lower stratospheric distributions of these trace gases [*Kawa et al.*, 1999].

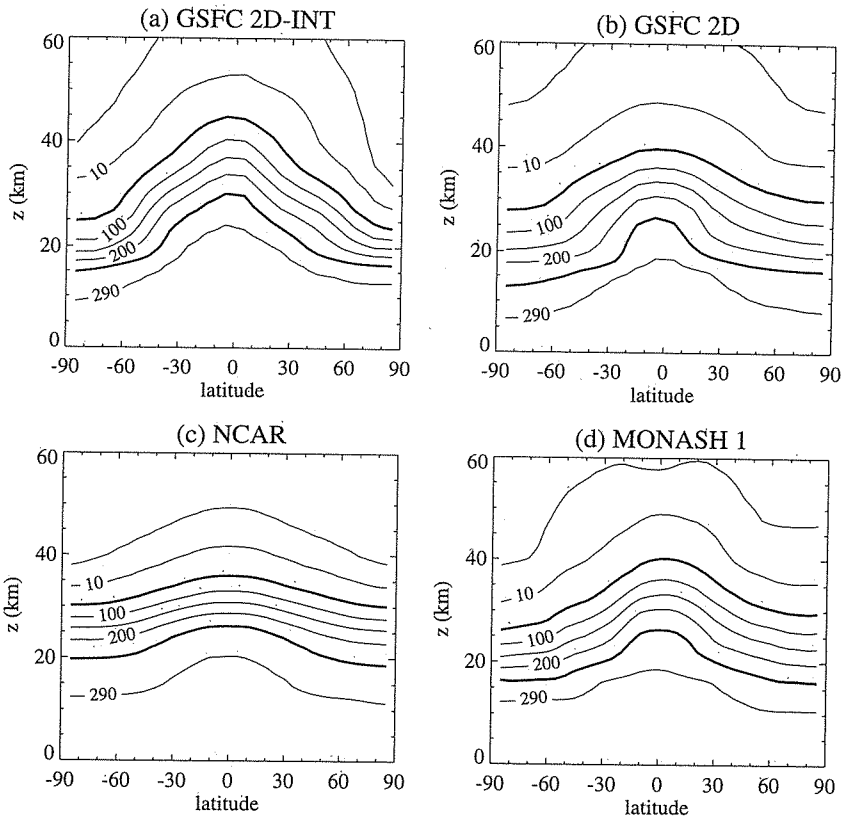

Figure 12. Annual mean zonal-mean N_2O distributions from same models as Figure 10. Contour intervals are 50 ppb, with additional contours shown for 1, 10, and 290 ppbv. (Adapted from *Hall et al.* [1999].)

[82] The correlation between mean age and photochemically active gases is not perfect, however. Using a 2-D model, *Li and Waugh* [1999] showed that changes in the transport that change the magnitude but not the shape of Γ isopleths (e.g., change in strength of the circulation, see section 4) have only a minor effect on the lower stratospheric concentrations of the N_2O and other chemically active trace gases. This insensitivity can be explained by the total "depletion" or "saturation" of the gas in the upper stratosphere and mesosphere. A stratospheric air parcel is made up of irreducible fluid elements that have taken a range of paths to the parcel location, and some of these paths have crossed through upper stratospheric and mesospheric regions of rapid photochemistry. Decreasing the circulation strength increases the mean age because all elements take longer to get to the parcel, including those that pass through upper levels. On the other hand, for these "high flying" elements, N_2O and other tracers with photochemical loss in upper stratosphere are fully depleted (i.e., nearly all N_2O is photolyzed) and Cl_y saturates (all available organic chlorine is converted to Cl_y). Additional time in the region results in no further change. Therefore the circulation strength has a larger impact on Γ than on chemical tracers for these irreducible elements.

[83] One might think that in a slower circulation less air passes through upper regions before returning to the troposphere, weakening or negating the above effect. However, an analysis of transport pathways by *Hall* [2000] indicates that the average maximum height achieved by air during its stratospheric residence is only weakly sensitive to the magnitude of circulation rates (e.g., tropical upwelling, tropical-extratropical mixing, and vertical diffusion), and so the total depletion/saturation effect does indeed limit the relationship between mean age and photochemical tracers.

[84] *Schoeberl et al.* [2000] also examined the relationship between age and long-lived tracers. Using a Lagrangian framework, they examined the dependence of the photochemical loss of irreducible elements on the pathway of the elements. They showed that elements with similar transit times experience similar photochemical loss, which means that the photochemical loss of an ensemble of elements with the same transit time can be calculated using the average path of the ensemble. They also showed, consistent with the above studies, a strong, but not perfect, correlation between mean age and long-lived tracers.

[85] Other trace gases of considerable interest are emissions from aircraft flying in the lower stratosphere, which may impact ozone chemistry [*Kawa et al.*, 1999]. A crucial aspect of the environmental impact of these emissions is their residence time τ_R in the stratosphere, defined as the steady state mass load divided by stratospheric source. The timescale τ_R is equivalent to the mean of the distribution of transit times for the tracer to

be transported from the source to the tropopause [*Hall and Waugh*, 2000]. Residence time and mean age are closely related. *Boering et al.* [1996] noted that Γ is proportional to a trace gas with uniform stratospheric source and tropospheric sink, as summarized in the ideal age equation (9). Furthermore, *Holzer and Hall* [2000] showed that the mean age at r is equivalent to τ_R for a source at r in the time-reversed adjoint flow. However, Γ and τ_R are not identical. Both are integrated measures of stratospheric transport that depend on a range of processes (e.g., advection by meridional circulation and mixing across transport "barriers"), but the two timescales weight the processes differently. This was illustrated by *Hall and Waugh* [2000], who examined the relationship between Γ and τ_R for an aircraft-like source in the lower-midlatitude stratosphere of the tropical leaky pipe model. Here τ_R and Γ are well correlated over a large range of circulations, but the correlation is not perfect. In particular, because the aircraft source is concentrated near the extratropical tropopause, τ_R is more sensitive to characteristics of this region, such as the tropopause height, than is Γ. The imperfect correlation between τ_R and Γ can also be seen in models of the MM2 study [see *Park et al.*, 1999, Figure 42, chapter 2; *Kawa et al.*, 1999, Figure 4–15]. *Hall and Waugh* [2000] concluded that models that underestimate Γ by large margins also underestimate the residence time of aircraft emissions, but models that underestimate Γ by only modest amounts could either underestimate or overestimate τ_R by modest amounts.

[86] Similar considerations apply to other trace gases of stratospheric source and tropospheric sink, such as H_2O produced from oxidation of CH_4 and H_2 in the stratosphere and mesosphere. The mean age may be useful in evaluating a model's ability to hold realistic amounts of H_2O from this source. In fact, the relationship between Γ and τ_R for H_2O from CH_4 and H_2 is likely stronger than that between Γ and aircraft emissions because the H_2O source is more spatially distributed and farther from the tropopause.

[87] As mentioned in section 3, a conserved family of chemicals whose abundance varies linearly in time has a distribution proportional to mean age. In fact, measurements of stratospheric Γ have been used to predict the total chlorine (Cl_{tot}) and bromine loading in the stratosphere from tropospheric measurements of the total abundances of chlorine and bromine [e.g., *Woodbridge et al.*, 1995; *Daniel et al.*, 1996; *Wamsley et al.*, 1998]. However, tropospheric total chlorine peaked around 1993–1994 and is now decreasing [*Montzaka et al.*, 1996], and using mean age to estimate the stratospheric loading during the current period when the temporal variation is nonlinear introduces some error. To illustrate this, the bold curves in Figure 13 show the "stratospheric" Cl_{tot} for three 1-D age spectra with the same mean age (6 years) but differing spectral width (see inset). For the narrow spectrum, there is very little difference between the time series and that using the mean age to lag the surface time series. However, for more realistic broader spectra, there is significant nonlinearity over the width of the age spectrum, and the two time series differ. In particular, the convolution over the spectrum results in a reduced peak in stratospheric Cl_{tot} and a more gradual turnover than at the surface (or inferred using the mean age as the time lag) [*Waugh et al.*, 2001]. Also shown in Figure 13 is the Cl_{tot} at 55 km estimated from HALOE HCl. As discussed by *Waugh et al.* [2001], the Cl_{tot} from HALOE turns over earlier and decays more rapidly than expected. The reason for this earlier decay is currently unknown.

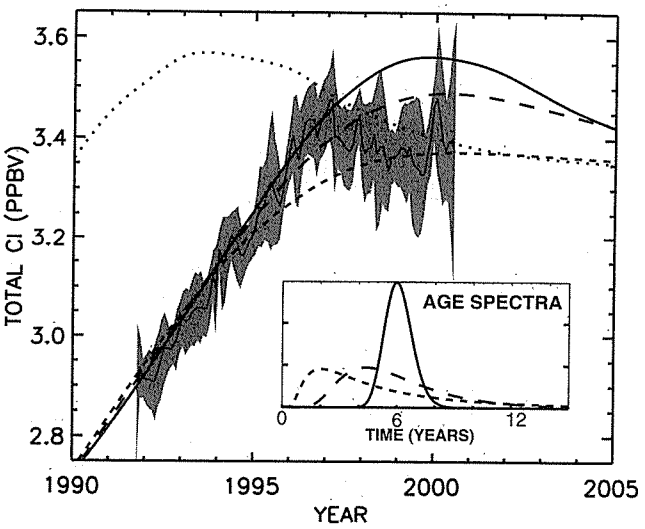

Figure 13. Time series of "stratospheric" total chlorine Cl_{tot} assuming different age spectra with mean age of 6 years but differing width (age spectra are shown in inset). Also shown are surface Cl_{tot} from the WMO [1999] "A1" scenario (dotted curve) and Cl_{tot} inferred from HALOE HCl at 55 km (thin curve is monthly and global mean values and shading represents 1-σ variation of the monthly averages). (Adapted from *Waugh et al.* [2001].)

6. CONCLUSIONS

[88] The use of "age" in stratospheric analysis has grown in recent years from a convenient empirical summary of sparse trace gas measurements to a component of a rigorous statistical description of stratospheric transport. Part of this description is the theory of transit time distributions (age spectra) and their relationship to observable transient tracers and stratospheric circulation. At the same time, there has been an enormous increase in aircraft, balloon, and satellite measurements of stratospheric tracers and from these measurements, there has been an increase in the number of estimates of the mean age and other transport timescales. In addition, many modelers have simulated mean age, both to understand better its diagnostic nature and to evaluate transport in their models by comparing to observations. The comparisons are stringent tests of model transport

and have highlighted certain problems with transport in current models (e.g., models generally underestimate the mean age and overattenuate propagating signals of annually repeating tracers). Age simulations and comparisons with data can now be considered standard tests of stratospheric models.

[89] There are, however, a number of outstanding issues with regard to our understanding and ability to model the mean age and age spectrum. Observationally, more complete spatial and temporal coverage of chronological tracers is needed to better define the mean age distribution. In particular, there are only a few measurements near the tropical tropopause. Additional observations are needed in this region to better define the concentration history of tracers entering the stratosphere and hence to reduce the uncertainty in mean age estimates.

[90] It is also important to infer from observations transport timescales complementary to mean age. This is true generally because transport cannot be summarized by a single timescale, and particularly because mean age weights heavily air that has resided for long times in the stratosphere, passing through regions of rapid photochemistry. Transport of this old air may not be as relevant for photochemically active trace gases as is younger air. The concentrations of these gases "saturate" in the old air even while the age keeps increasing. Thus, although mean age is a powerful transport diagnostic, its sensitivity to old air imposes a limit on its relationship to active trace gases. More inferences of timescales that preferentially weight younger air, such as periodic tracers, are needed to complement mean age observations.

[91] The full age spectrum represents transport information at all timescales, and knowledge of it would circumvent the old air sensitivity problem of the mean age. In this regard the recent estimates of the age spectra from CO_2 observations by *Andrews et al.* [1999, 2001a] are of particular interest. To improve such age spectral estimates, however, additional observations and analyses are necessary. More CO_2 measurements would be especially useful to corroborate and better define the midlatitude bimodal spectra. With sufficient observations it may be possible to track the propagation into the stratosphere of interannual CO_2 variations, which would complement the linear trend and annual cycle. Other tracers, yet to be exploited, offer the possibility of independent constraints on the spectrum. For example, the growth of CFC replacement gases may be nonlinear enough to sample early components of the age spectrum disproportionately, thereby representing independent constraints compared to the quasi-linear tracers CO_2 and SF_6. Preliminary analysis indicates that stratospheric measurements of HFC-134a made between 1995 and 2000 [*Schauffler et al.*, 1999] contain information on the shape (width) of the age spectra.

[92] Even if the full age spectrum were known at a given location, it would still provide no information itself about transport pathways. However, coupled with kinematic models, observational inferences about the age spectrum can be used to infer pathways. *Andrews et al.* [2001a] argue that CO_2 measurements imply a bimodal age spectrum in the midlatitude lower stratosphere and associate the early peak with direct transport from the tropics and the later peak with "up and over" transport of the Brewer-Dobson circulation. Further tracer analyses are needed to corroborate these results. Distinct pathways should, in principle, leave a signature in long-lived photochemically active species as well, such as N_2O. Assuming sufficient knowledge of the photochemistry, it may be possible to invert the active trace gas distribution and infer pathways and aspects of the age spectrum, similar to a suggestion by *Schoeberl et al.* [2000].

[93] Finally, more work is needed to sort out the causes of numerical model discrepancies in mean age and annual cycle propagation compared to observations. It is not at present possible to state generally which erroneous features are caused by which inaccuracies in model dynamics. Both large-scale features of the circulation and numerical diffusion and dispersion appear to have a role in influencing mean age [*Hall et al.*, 1999; *Eluszkiewicz et al.*, 2000]. Nor can these aspects of a model's transport be completely separated, particularly in three dimensions, as numerical diffusion acts to distribute active trace gases, which, in turn, influence the circulation. The fact that different dynamical and numerical processes can cause similar inaccuracies in mean age simulations, depending on the nature of the model (2-D versus 3-D and off-line CTM versus on-line GCM), suggests that using independent tracers in combination to evaluate and improve models is the best approach.

[94] **ACKNOWLEDGEMENTS.** We thank Arlyn Andrews for providing Figure 8, Kristie Boering for Figure 9, and Janusz Eluszkiewicz, Tom Haine, Kevin Hamilton, Dale Hurst, and Alan Plumb for helpful comments on earlier versions of the manuscript. This work was supported by the NASA Atmospheric Chemistry and Modeling Program.

Kendal McGuffie was the Editor responsible for this paper. He thanks two anonymous technical reviewers.

REFERENCES

Anderson, J., J. M. Russell III, S. Solomon, and L. Deaver, Halogen Occultation Experiment confirmation of stratospheric chlorine decreases in accordance with the Montreal Protocol, *J. Geophys. Res.*, *105*, 4483–4490, 2000.

Andrews, A. E., K. A. Boering, B. C. Daube, and S. C. Wofsy, Empirical age spectra from observations of stratospheric CO_2: Mean ages, vertical asecent rates, and dispersion in the lower tropical stratosphere, *J. Geophys. Res.*, *104*, 26,581–26,595, 1999.

Andrews, A. E., et al., Empirical age spectra for the midlatitude lower stratosphere from in situ observations of CO_2: Quantitative evidence for a subtropical "barrier" to horizontal transport, *J. Geophys. Res.*, *106*, 10,257–10,274, 2001a.

Andrews, A. E., et al., Mean ages of stratospheric air derived from in situ observations of CO_2, CH_4, and N_2O, *J. Geophys. Res.*, *106*, 32,295–32,314, 2001b.

Andrews, D. G., J. R. Holton, and C. B. Leovy, *Middle Atmosphere Dynamics*, 489 pp., Academic, San Diego, Calif., 1987.

Bacmeister, J. T., et al., Age of air in a zonally averaged two-dimensional model, *J. Geophys. Res.*, *103*, 11,263–11,288, 1998.

Beining, P., and W. Roether, Temporal evolution of CFC 11 and CFC 12 concentrations in the ocean interior, *J. Geophys. Res.*, *101*, 16,455–16,464, 1996.

Bischof, W., et al., Increased concentration and vertical distribution of carbon dioxide in the stratosphere, *Nature*, *316*, 708–710, 1985.

Boering, K. A., B. C. Daube, S. C. Wofsy, M. Loewenstein, J. R. Podolske, and E. R. Keim, Tracer-tracer relationships and lower stratospheric dynamics: CO_2 and N_2O correlations during SPADE, *Geophys. Res. Lett.*, *21*, 2567–2570, 1994.

Boering, K. A., et al., Measurements of stratospheric carbon dioxide and water vapor at northern midlatitudes: Implications for troposphere-to-stratosphere transport, *Geophys. Res. Lett.*, *22*, 2737–2740, 1995.

Boering, K. A., et al., Stratospheric transport rates and mean age distribution derived from observations of atmospheric CO_2 and N_2O, *Science*, *274*, 1340–1343, 1996.

Bolin, B., and H. Rhode, A note on the concepts of age distribution and transit time in natural reservoirs, *Tellus*, *25*, 58–62, 1973.

Boville, B. A., Middle atmosphere version of the CCM2 (MACCM2): Annual cycle and interannual variability, *J. Geophys. Res.*, *100*, 9017–9039, 1995.

Brewer, A. W., Evidence for a world circulation provided by the measurements of helium and water vapour distribution in the stratosphere, *Q. J. R. Meteorol. Soc.*, *75*, 351–363, 1949.

Chhikara, R. S., and J. L. Folks, *The Inverse Gaussian Distribution: Theory, Methodology and Applications*, Marcel Dekker, New York, 1989.

Conway, T. J., P. P. Tans, L. S. Waterman, K. W. Thoning, D. R. Kitzis, K. A. Masarie, and N. Zhang, Evidence for interannual variability of the carbon cycle from the National Oceanic and Atmospheric Administration/Climate Monitoring and Diagnostics Laboratory Global Air Sampling Network, *J. Geophys. Res.*, *99*, 22,831–22,855, 1994.

Danckwerts, P. V., Continuous flow systems, *Chem. Eng. Sci.*, *38*, 1–4, 1953.

Daniel, J. S., S. M. Schauffler, W. A. Pollock, S. Solomon, A. Weaver, L. E. Heidt, R. R. Garcia, E. L. Atlas, and J. F. Vedder, On the age of stratospheric air and inorganics chlorine and bromine release, *J. Geophys. Res.*, *101*, 16,757–16,770, 1996.

Deleersnijder, E., J. Campin, and E. J. M. Delhez, The concept of age in marine modeling, I, Theory and preliminary model results, *J. Mar. Res.*, *29*, 229–267, 2001.

Dobson, G. M. B., Origin and distribution of the polyatmoic molecules in the atmosphere, *Proc. R. Soc. London, Ser. A*, *236*, 187–193, 1956.

Ehhalt, D. H., F. Rohrer, S. Schauffler, and W. Pollock, Tritiated water vapor in the stratosphere: Vertical profiles and residence time, *J. Geophys. Res.*, doi:2001JD001343, in press, 2002.

Elkins, J. W., et al., Airborne gas chromatograph for in situ measurements of long-lived species in the upper troposphere and lower stratosphere, *Geophys. Res. Lett.*, *23*, 347–350, 1996.

Eluszkiewicz, J., et al., Residual circulation in the stratosphere and lower mesosphere as diagnosed from microwave limb sounder data, *J. Atmos. Sci.*, *53*, 217–240, 1996.

Eluszkiewicz, J., R. S. Hemler, J. D. Mahlman, L. Bruhwiler, and L. L. Takacs, Sensitivity of age-of-air calculations to the choice of advection scheme, *J. Atmos. Sci.*, *57*, 3185–3201, 2000.

England, M. H., The age of water and ventilation timescales in a global ocean model, *J. Phys. Oceanogr.*, *25*, 2756–2777, 1995.

Eriksson, E., Compartment models and reservoir theory, *Annu. Rev. Ecol. Syst.*, *2*, 67–84, 1971.

Etcheverry, D., and P. Perrochet, Direct simulation of groundwater transit-time distribution using the reservoir theory, *Hydrogeol. J.*, *8*, 200–208, 2000.

Fleming, E. L., C. H. Jackman, R. S. Stolarski, and D. B. Considine, Simulation of stratospheric tracers using an improved empirically based two-dimensional model transport formulation, *J. Geophys. Res.*, *104*, 23,911–23,934, 1999.

Garcia, R. R., F. Stordal, S. Solomon, and J. T. Kiehl, A new numerical model of the middle atmosphere, I, Dynamics and transport of tropospheric source gases, *J. Geophys. Res.*, *97*, 12,967–12,991, 1992.

Geller, L. S., J. W. Elkins, R. C. Myers, J. M. Lobert, A. D. Clarke, D. F. Hurst, and J. H. Butler, Tropospheric SF_6: Observed latitudinal distribution and trends, derived emissions, and interhemispheric exchange time, *Geophys. Res. Lett.*, *24*, 675–678, 1997.

Goode, D. J., Direct simulation of groundwater age, *Water Resour. Res.*, *32*, 289–296, 1996.

Grant, W. B., E. V. Browell, C. S. Long, and L. L. Stowe, Use of aerosols from volcanic eruptions to study the tropical stratospheric reservoir, its boundary, and transport to northern midlatitudes, *J. Geophys. Res.*, *101*, 3973–3988, 1996.

Gunson, M. R., et al. The Atmospheric Trace Molecule Spectroscopy (ATMOS) experiment: Deployment on the ATLAS Space Shuttle missions, *Geophys. Res. Lett.*, *23*, 2333–2336, 1996.

Haine, T. W. N., and T. M. Hall, A generalized transport theory: Water-mass composition and age, *J. Phys. Oceanogr.*, *32*, 1932–1946, 2002.

Hall, T. M., Path histories and timescales in stratospheric transport: Analysis of an idealized model, *J. Geophys. Res.*, *105*, 22,811–22,823, 2000.

Hall, T. M., and T. W. N. Haine, A note on ocean transport diagnostics: Ideal age and the age spectrum, *J. Phys. Oceanogr.*, *32*, 1987–1991, 2002.

Hall, T. M., and R. A. Plumb, Age as a diagnostic of stratospheric transport, *J. Geophys. Res.*, *99*, 1059–1070, 1994.

Hall, T. M., and M. J. Prather, Simulations of the trend and annual cycle in stratospheric CO_2, *J. Geophys. Res.*, *98*, 10,573–10,581, 1993.

Hall, T. M., and D. W. Waugh, Timescales for the stratospheric circulation derived from tracers, *J. Geophys. Res.*, *102*, 8991–9001, 1997a.

Hall, T. M., and D. W. Waugh, Tracer transport in the tropical stratosphere due to vertical diffusion and horizontal mixing, *Geophys. Res. Lett.*, *24*, 1383–1387, 1997b.

Hall, T. M., and D. W. Waugh, Influence of nonlocal chemistry on tracer distributions: Inferring the mean age of air from SF6, *J. Geophys. Res.*, *103*, 13,327–13,336, 1998.

Hall, T. M., and D. W. Waugh, Stratospheric residence time and its relationship to mean age, *J. Geophys. Res.*, *105*, 6773–6782, 2000.

Hall, T. M., D. W. Waugh, K. A. Boering, and R. A. Plumb, Evaluation of transport in stratospheric models, *J. Geophys. Res.*, *104*, 18,815–18,839, 1999.

Hall, T. M., T. W. N. Haine, and D. W. Waugh, Inferring the concentration of anthropogenic carbon in the ocean from

tracers, *Global Biogeochem. Cycles*, *16*(4), 1131, doi: 10.1029/2001GB001835, 2002.

Harnisch, J., R. Borchers, P. Fabian, and M. Maiss, Tropospheric trends for CF_4 and C_2F_6 since 1982 derived from SF_6 dated stratospheric air, *Geophys. Res. Lett.*, *23*, 1099–1102, 1996.

Harnisch, J., W. Bischof, R. Borchers, P. Fabian, and M. Maiss, A stratospheric excess of CO_2-due to tropical deep convection?, *Geophys. Res. Lett.*, *25*, 63–66, 1998.

Harnisch, J., R. Borchers, P. Fabian, and M. Maiss, CF_4 and the age of mesospheric and polar vortex air, *Geophys. Res. Lett.*, *26*, 295–298, 1999.

Herman, R. L., et al., Tropical entrainment time scales inferred from stratospheric N_2O and CH_4 observations, *Geophys. Res. Lett.*, *25*, 2781–2784, 1998.

Holton, J. R., A dynamically based transport parameterization for one-dimensional photochemical models of the stratosphere, *J. Geophys. Res.*, *91*, 11,625–11,640, 1986.

Holton, J. R., P. H. Haynes, M. E. McIntyre, A. R. Douglass, R. B. Rood, and L. Pfister, Stratosphere—troposphere exchange, *Rev. Geophys.*, *33*, 403–439, 1995.

Holzer, M., and T. M. Hall, Transit-time and tracer-age distributions in geophysical flows, *J. Atmos. Sci.*, *57*, 3539–3558, 2000.

Johnson D. G., et al., Stratospheric age spectra derived from observations of water vapor and methane, *J. Geophys. Res.*, *104*, 21,595–21,602, 1999.

Jost, H., et al., Filaments in the tropical middle atmosphere: Origin and age estimates, *Geophys. Res. Lett.*, *25*, 4337–4340, 1998.

Kawa, S. R., J. Anderson, C. Brock, R. Cohen, D. Kinnison, P. A. Newman, J. Rodriguez, R. Stolarksi, D. W. Waugh, and S. Wofsy, Assessment of the effects of high-speed aircraft in the stratosphere: 1998, *NASA Tech. Publ., 1999–209236*, 1999.

Khatiwala, S., et al., Age tracers in an ocean GCM, *Deep Sea Res., Part I*, *48*, 1423–1441, 2001.

Kida, H., General circulation of air parcels and transport characteristics derived from a hemispheric GCM, Part 2, Very long-term motions of air parcels in the troposphere and stratosphere, *J. Meteorol. Soc. Jpn.*, *61*, 510–522, 1983.

Levenspiel, O., *Chemical Reaction Engineering*, 578 pp., John Wiley, New York, 1972.

Li, S., and D. W. Waugh, Sensitivity of mean age and long-lived tracers to transport coefficients in two-dimensional models, *J. Geophys. Res.*, *104*, 30,559–30,569, 1999.

Lin, S. J., and R. B. Rood, Multidimensional flux-form semi-Lagrangian transport schemes, *Mon, Weather Rev.*, *124*, 2046–2070, 1996.

Mahlman, J. D., H. Levy, and W. J. Moxim, Three-dimensional simulations of stratospheric N_2O: Predictions for other trace constituents, *J. Geophys. Res.*, *91*, 2687–2707, 1986.

Mahowald, N. M., R. A. Plumb, P. J. Rasch, J. del Corral, F. Sassi, and W. Heres, Stratospheric transport in a three-dimensional isentropic coordinate model, *J. Geophys. Res.*, *107*(D15), 4254, doi:10.1029/2001JD001313, 2002.

Maiss, M., et al., Sulfur hexafluoride: A powerful new atmospheric tracer, *Atmos. Environ.*, *30*, 1621–1629, 1996.

Manzini, E., and J. Feichter, Simulation of the SF_6 tracer with the middle atmosphere MAECHAM4 model: Aspects of the large-scale transport, *J. Geophys. Res.*, *104*, 31,097–31,108, 1999.

McIntyre, M. E., and T. N. Palmer, Breaking planetary waves in the stratosphere, *Nature*, *305*, 593–600, 1983.

Montzaka, S. A., et al., Decline in the tropospheric abundance of halogen from halocarbons: Implications for stratospheric ozone depletion, *Science*, *272*, 1318–1322, 1996.

Morris, R. A., et al., Effects of electron and ion reactions on atmospheric lifetimes of fully fluorinated compounds, *j. Geophys. Res.*, *100*, 1287–1294, 1995.

Mote, P. W., et al., An atmospheric tape recorder: The imprint of tropical tropopause temperatures on stratospheric water vapor, *J. Geophys. Res.*, *101*, 3989–4006, 1996.

Mote, P. W., T. J. Dunkerton, M. E. Mc Intyre, E. A. Ray, P. H. Haynes, and J. M. Russell III, Vertical velocity, vertical diffusion, and dilution by midlatitude air in the tropical lower stratosphere, *J. Geophys. Res.*, *103*, 8651–8666, 1998.

Murphy, D. M., D. W. Fahey, M. H. Proffitt, S. C. Liu, K. R. Chan, C. S. Eubank, S. R. Kawa, and K. K. Kelly, Reactive nitrogen and its correlation with ozone in the lower stratosphere and upper troposphere, *J. Geophys. Res.*, *98*, 8751–8773, 1993.

Nakazawa, T., T. Machida, S. Sugawara, S. Murayama, S. Morimoto, G. Hashida, H. Honda, and T. Itoh, Measurements of the stratospheric carbon dioxide concentration over Japan using a balloon-borne cryogenic sampler, *Geophys. Res. Lett.*, *22*, 1229–1232, 1995.

Nedoluha, G. E., D. E. Siskind, J. T. Bacmeister, R. M. Bevilacqua, and J. M. Russell, Changes in upper stratospheric CH_4 and NO_2 as measured by HALOE and implication for changes in transport, *J. Geophys. Res.*, *103*, 3531–3543, 1998.

Neu, J. L., and R. A. Plumb, Age of air in "leaky pipe" model of stratospheric transport, *J. Geophys. Res.*, *104*, 19,243–19,255, 1999.

Nir, A., and S. Lewis, On tracer theory in geophysical systems in the steady and non-steady state, 1, *Tellus*, *27*, 372–383, 1975.

O'Neill, B. C., S. R. Gaffin, F. M. Tubiello, and M. Oppenheimer, Reservoir timescales for anthropogenic CO_2 in the atmosphere, *Tellus, ser. B*, *46*, 378–389, 1994.

Park, J., et al., The atmosphere effects of stratospheric aircraft: Reports of the 1998 Models and Measurements II workshop, *NASA Tech. Memo., 1991–209554*, 1999.

Patra, P. K., et al., Observed vertical profile of sulfur hexafluoride (SF_6) and its atmospheric applications, *J. Geophys. Res.*, *102*, 8855–8859, 1997.

Plumb, I. C., P. F. Vohralik, and K. R. Ryan, Normalization of correlations for atmospheric species with chemical loss, *J. Geophys. Res.*, *104*, 11,723–11,732, 1999.

Plumb, R. A., A tropical pipe model of stratospheric transport, *J. Geophys. Res.*, *101*, 3957–3972, 1996.

Plumb, R. A. and M. K. W. Ko, Interrelationships between mixing ratios of long-lived stratospheric constituents, *J. Geophys. Res.*, *97*, 10,145–10,156, 1992.

Plumb, R. A., et al., Global tracer modeling during SOLVE: High-latitude descent and mixing, *J. Geophys. Res.*, *107*, 8309, doi:10.1029/2001JD001023, 2002. [printed *108* (D5), 2003].

Prather, M. J., Numerical advection by conservation of second-order moments, *j. Geophys. Res.*, *91*, 6671–6681,1986.

Prather, M. J., Timescales in atmospheric chemistry: CH_3Br, the ocean, and ozone depletion potentials, *Global Biogeochem. Cylcles*, *11*, 393–400, 1997.

Randel, W. J., B. A. Boville, J. C. Gille, P. L. Bailey, S. T. Massie, J. B. Kumer, J. L. Mergenthaler, and A. E. Roche, Simulation of stratospheric N_2O in the NCAR CCM2: Comparison with CLAES data and global budget analyses, *J. Atmos. Sci.*, *51*, 2834–2845, 1994.

Randel, W. J., F. Wu. J. M. Russell, and J. W. Waters, Space-time patterns of trends in stratospheric constituents derived from UARS measurements, *J. Geophys. Res.*, *104*, 3711–3727, 1999.

Rasch, P. J., and D. L. Williamson, On shape-preserving interpolation and semi-Lagrangian transport, *SIAM, J. Sci. Stat. Comput.*, *11*, 656–687, 1990.

Ravishankara, A. R., S. Solomon, A. A. Turnipseed, and R. F. Warren, Atmospheric lifetimes of long-lived halogenated species, *Science*, *259*, 194–199, 1993.

Ray, E. A., et al., Transport into the Northern Hemisphere lowermost stratosphere revealed by in situ tracer measurements, *J. Geophys. Res.*, *104*, 26,565–26,580, 1999.

Reddmann, T., R. Ruhnke, and W. Kouker, Three-dimensional model simulations of SF_6 with mesospheric chemistry, *J. Geophys. Res.*, *106*, 14,525–14,537, 2001.

Rosenfield, J. E., D. B. Considine, P. E. Meade, J. T. Bacmeister, C. H. Jackman, and M. R. Schoeberl, Stratospheric effects of Mount Pinatubo aerosol studies with a coupled two-dimensional model, *J. Geophys. Res.*, *102*, 3649–3670, 1997.

Rosenlof, K. H., Seasonal cycle of the residual mean circulation in the stratosphere, *J. Geophys. Res.*, *100*, 5173–5191, 1995.

Russell, J. M., M. Luo, R. J. Cicerone, and L. E. Deaver, Satellite confirmation of the dominance of chlorofluorocarbons in the global stratospheric chlorine budget, *Nature*, *379*, 526–529, 1996.

Schauffler, S. M., E. L. Atlas, D. R. Blake, F. Flocke, R. A. Lueb, J. M. Lee-Taylor, V. Stroud, and W. Travnicek, Distributions of brominated organic compounds in the troposphere and lower stratosphere, *J. Geophys. Res.*, *104*, 21,513–21,535, 1999.

Schmidt, U., and A. Khedim, In situ measurements of carbon dioxide in the winter arctic vortex and at midlatitudes: An indicator of the age of stratospheric air, *Geophys. Res. Lett.*, *18*, 763–766, 1991.

Schoeberl, M. R., L. Sparling, A. Dessler, C. H. Jackman, and E. L. Fleming, A Lagrangian view of stratospheric trace gas distributions, *J. Geophys. Res.*, *105*, 1537–1552, 2000.

Sen, B., G. C. Toon, J.-F. Blavier, E. F. Flemins, and C. H. Jackman, Balloon-borne observations of midlatitude fluorine abundance, *J. Geophys. Res.*, *101*, 9045–9054, 1996.

Seshadri, V., *The Inverse Gaussian Distribution*, Springer-Verlag, New York, 1999.

Shindell, D., D. Rind, and P. Lonergan, Increased polar stratospheric ozone losses and delayed eventual recovery owing to increasing greenhouse-gas concentrations, *Nature*, *392*, 589–592, 1998.

Strunk, M., A. Engel, H. Schmidt, C. M. Volk, T. Wetter, I. Levin, and H. Glatzel-Matteier, CO_2 and SF_6 as stratospheric age tracers: Consistency and the effect of mesospheric SF_6-loss, *Geophys. Res. Lett.*, *25*, 341–344, 2000.

Thiele, G., and J. L. Sarmiento, Tracer dating and ocean ventilation, *J. Geophys. Res.*, *95*, 9377–9391, 1990.

Trepte, C. R., R. E. Viega, and M. P. McCormick, The poleward dispersal of Mount Pinatubo volcanic aerosol, *J. Geophys. Res.*, *98*, 18,563–18,574, 1993.

Varni, M., and J. Carrera, Simulation of groundwater age distributions, *Water Resour. Res.*, *34*, 3271–3281, 1998.

Volk, C. M., et al., Quantifying transport between the tropics and middle latitudes in the lower stratosphere, *Science*, *272*, 1763–1768, 1996.

Volk, C. M., et al., Evaluation of source gas lifetimes from stratospheric observations, *J. Geophys. Res.*, *102*, 25,543–25,564, 1997.

Volz, A., D. H. Ehhalt, A. Khedim, and A. Schmidt, Vertical profiles of CO_2 in the stratosphere, in *Proceedings of the Quadrennial International Ozone Symposium*, vol. 2, edited by J. London, pp. 824–828, Int. Ozone Comm., Int. Assoc. of Meteorol. and Atmos. Phys., Boulder, Colo., 1981.

Wamsley, P. R., et al., Distribution of halon-1211 in the upper troposphere and lower stratosphere and the 1994 total bromine budget, *J. Geophys. Res.*, *103*, 1513–1526, 1998.

Waugh, D. W., et al., Three-dimensional simulations of long-lived tracers using winds from MACCM2, *J. Geophys. Res.*, *102*, 21, 493–513, 1997.

Waugh, D. W., D. B. Considine, and E. L. Fleming, Is stratospheric chlorine decreasing as expected?, *Geophys. Res. Lett.*, *28*, 1187–1190, 2001.

Weinstock, E. M. et al., Constraints on the seasonal cycle of stratospheric water vapor using in situ measurements from the ER-2 and a CO photochemical clock, *J. Geophys. Res.*, *106*, 22,707–22,724, 2001.

Woodbridge, E. L., et al. Estimates of total organic and inorganic chlorine in the lower stratosphere from in situ and flask measurements during AASE II, *J. Geophys. Res.*, *100*, 3057–3064, 1995.

World Meteorological Organization, Scientific assessment of ozone depletion: 1998, *WMO Rep.* 20, U. N. Environ. Programme, Geneva, Switzerland, 1999.

Yudin, V. A., S. P. Smyshlyaev, M. A. Geller, and V. L. Dvortsov, Transport diagnostics of GCMs and implications for 2D chemical-transport models of troposphere and stratosphere, *J. Atmos. Sci.*, *57*, 673–699, 2000.

Zander, R., et al., The 1994 northern midlatitude budget of stratospheric chlorine derived from ATMOS/ATLAS-3 observations, *Geophys. Res. Lett.*, *23*, 2357–2360, 1996.

Zhu, X., J.-H. Yee, and D. F. Strobel, Middle atmosphere age of air in a globally balanced two-dimensional model, *J. Geophys. Res.*, *105*, 15,201–15,212, 2000.

T. M. Hall, NASA Goddard Institute for Space Studies, 2880 Broadway, New York, NY 10025, USA. (thall@giss.nasa.gov)

D. W. Waugh, Department of Earth and Planetary Science, Johns Hopkins University, Baltimore, MD 21218, USA. (waugh@jhu.edu)